

ROM SAF Report 14
Ref: SAF/ROM/METO/REP/RSR/014
Web: www.romsaf.org
Date: 16 Oct 2013

The EUMETSAT
Network of
Satellite
Application
Facilities



ROM SAF Report 14

A review of the geodesy calculations in ROPP

Ian Culverwell

Met Office, Exeter, UK

Document Author Table

	<i>Name</i>	<i>Function</i>	<i>Date</i>	<i>Comments</i>
Prepared by:	I. D. Culverwell	ROM SAF Project Team	16 Oct 2013	
Reviewed by:	D. Offiler	ROM SAF Project Team	27 Feb 2013	
Reviewed by:	J. R. Eyre	ROM SAF Steering Group Member	13 May 2013	
Approved by:	K. B. Lauritsen	ROM SAF Project Manager	26 Sep 2013	

Document Change Record

<i>Issue/Revision</i>	<i>Date</i>	<i>By</i>	<i>Description</i>
1st draft	25 Feb 2013	IDC	First draft, based on report attached to ROPP ticket 159
2nd draft	27 Mar 2013	IDC	Corrections following 1st review by DO
Version 1.0	11 Sep 2013	IDC	Amendments after contacting ROPP-2.0 beta reviewer

ROM SAF

The Radio Occultation Meteorology Satellite Application Facility (ROM SAF) is a decentralised processing centre under EUMETSAT which is responsible for operational processing of GRAS radio occultation data from the Metop satellites and RO data from other missions. The ROM SAF delivers bending angle, refractivity, temperature, pressure, and humidity profiles in near-real time and offline for NWP and climate users. The offline profiles are further processed into climate products consisting of gridded monthly zonal means of bending angle, refractivity, temperature, humidity, and geopotential heights together with error descriptions.

The ROM SAF also maintains the Radio Occultation Processing Package (ROPP) which contains software modules that will aid users wishing to process, quality-control and assimilate radio occultation data from any radio occultation mission into NWP and other models.

The ROM SAF Leading Entity is the Danish Meteorological Institute (DMI), with Cooperating Entities: i) European Centre for Medium-Range Weather Forecasts (ECMWF) in Reading, United Kingdom, ii) Institut D'Estudis Espacials de Catalunya (IEEC) in Barcelona, Spain, and iii) Met Office in Exeter, United Kingdom. To get access to our products or to read more about the project please go to: <http://www.romsaf.org>

Intellectual Property Rights

All intellectual property rights of the ROM SAF products belong to EUMETSAT. The use of these products is granted to every interested user, free of charge. If you wish to use these products, EUMETSAT's copyright credit must be shown by displaying the words "copyright (year) EUMETSAT" on each of the products used.

Abstract

This report reviews the geodesy calculations in ROPP, in response to concerns raised by the ROPP2.0 beta reviewer in 2008. Various expressions for the surface gravity, effective radius, radius of curvature and geopotential height are compared, and the impact of the differences in RO applications is assessed. Supporting sensitivity studies are reported. A simple model is developed that sheds light on some of the findings.

Contents

1	Introduction	5
2	Gravity	6
2.1	Variation with latitude	6
2.2	Variation with altitude	10
3	Effective radius of Earth	11
4	Geopotential height	14
5	Radius of curvature	16
6	Undulation	20
7	Response to ROPP2.0 beta reviewer's comments	22
8	Sensitivity studies	24
8.1	Sensitivity to surface gravity	24
8.2	Sensitivity to effective radius	27
8.3	Sensitivity to radius of curvature	29
8.4	Sensitivity to undulation	31
9	Summary and conclusions	33
10	Appendix: The geodesy of Rodworld	35
10.1	Intoduction	35
10.2	Absence of rotation	35
10.2.1	Geopotential	36
10.2.2	Surface gravity	36
10.2.3	Effective radius	37
10.3	Presence of rotation	40
10.3.1	Geopotential	40
10.3.2	Surface gravity	40
10.3.3	Effective radius	41
10.4	Summary	41
	Bibliography	43

1 Introduction

Geodesy is the study of the measurement and representation of the Earth, including its gravitational field. A review of the geodesy calculations in ROPP was suggested by the ROPP2.0 beta reviewer ([1]). His concerns were that these calculations are not being done sufficiently accurately and/or consistently in ROPP, and he suggested that the treatment of geodetic terms should be re-examined.

There were two main aspects to the reviewer's concern: insufficient accuracy in the transformation between geometric and geopotential height, and the apparent inconsistency between the effective radius of the Earth and the radius of curvature of the Earth at the tangent point.

Lewis ([6]) compared the early ROPP implementations of gravity, effective radius and geopotential, based on expressions in the Smithsonian Meteorological Tables ([14]), and versions which have since been implemented in ROPP, based on Mahoney's ([8]) calculations using Somigliana's equation. He found that the fractional differences between the calculations of gravity and of geopotential were negligible ($< 10^{-5}$), but that the fractional difference in effective radius of 5×10^{-5} equated to 350 m, which was considered excessive. This is why ROPP has consistently used geodesy routines based on Somigliana's equation since ROPP1.2.

A follow-up note (Lewis 2010 pers. comm.) discussed the differences between these later expressions for gravity, effective radius and geopotential and those used in the *Invert* package, which is used to process ROM SAF NRT products. He found various inconsistencies between the two sets of expressions: a 3×10^{-5} fractional difference in the equatorial gravity, and up to 300 m difference in effective radius. The differences in geopotential height were generally less than 1 m, however, and therefore considered negligible.

The treatment of the radius of curvature in ROPP has developed since ROPP2.0 was reviewed, and, as the reviewer recommended, expressions involving the true radius of curvature of the section of the ellipsoid intersected by the occultation plane are now used in the `ropp_utils/coordinates` routines that are used by the `ropp_pp` module of ROPP.

This report attempts to tie all these threads together, and give a coherent account of the current geodesy calculations in ROPP.

Throughout the following discussion of the wide range of available geodesy calculations it should be borne in mind that ROPP itself is internally consistent: all modules use common expressions for geodesic parameters and formulae which are held in the `ropp_utils` module. This is one of the strengths of the modular structure of ROPP.

Geodesy is important to radio occultation in two distinct ways: "physically", in connection with the effects of gravity on the atmosphere; and "mathematically", in connection with the natural co-ordinate system in which to discuss the bending of radio signals during an occultation. These two facets will be discussed separately, before being brought together.

2 Gravity

2.1 Variation with latitude

Numerous expressions for the Earth's gravity field appear in the literature.

The most authoritative reference appears to be the International Gravity Formula (Lambert 1945 [4]). Writing $g(h, \phi)$ for the effective (ie including rotational effects) gravity at geometric height h and geographic (or geodetic) latitude ϕ^1 , Lambert gives the surface gravity as

$$\text{Lambert: } g(0, \phi) = g_{\text{eq}}(1 + \beta \sin^2 \phi - \beta_1 \sin^2 2\phi) \quad (2.1)$$

where (ignoring third order terms and some geometric shape factors like everyone else)

$$\beta = (5/2)m - f - (17/14)mf \approx 5.3 \times 10^{-3} \quad (2.2)$$

and

$$\beta_1 = (f/8)(f + 2\beta) = (f/8)(5m - f) \approx 5.9 \times 10^{-6}. \quad (2.3)$$

Here, $g_{\text{eq}} = g(0, 0)$ is surface gravity at equator, $f = (a - c)/a$ is the flattening of the oblate ellipsoid which is assumed to be described by the mean sea level geoid² with semi-major and semi-minor axes a and c respectively, and $m = \omega^2 a / g_{\text{eq}}$ is the ratio of centrifugal to gravitational force on the equator. For the Earth, not coincidentally³, f and m are numerically similar: $f \approx m \approx 1/300$. This makes $\beta > 0$, which implies (since $\beta \gg \beta_1$) that g increases towards the poles, as might be expected from both the reduced centrifugal "dilution" of gravity (m) and the smaller distance to the Earth's centre (f). A glance at Eqn (2.2) shows that only one of these statements is true. More on this later.

Numerically in Eqn (2.1):

$$g_{\text{eq}} = 9.7803253359 \text{ ms}^{-2}; \quad \beta = 5.3024396 \times 10^{-3}; \quad \beta_1 = 5.8496912 \times 10^{-6}. \quad (2.4)$$

Eqn (2.1), or something very much like it, appears throughout the literature (eg [14], [8]).

Somigliana's equation for the surface gravity, as currently used in ROPP (`ropp_utils/geodesy/gravity.f90`), takes the form ([2]):

$$\text{Somigliana: } g(0, \phi) = g_{\text{eq}}(1 + k_s \sin^2 \phi) / \sqrt{1 - e^2 \sin^2 \phi} \quad (2.5)$$

¹That is, the angle between the local vertical and the equatorial plane. (As opposed to the geocentric latitude, which is the angle between the radius vector from the Earth's centre to the given point and the equatorial plane.)

²But see Section 6 for a discussion of the undulation.

³In *Principia Mathematica*, Newton derived $f = 5m/4$ for a uniformly rotating homogeneous blob of fluid (reported by White et al [16]). The non-uniform density of the Earth means that in practice f is rather closer to m .

where

$$k_s(\text{Somigliana's constant}) = (cg_{po} - ag_{eq})/ag_{eq} \approx 1.9 \times 10^{-3} \quad (2.6)$$

and

$$e(\text{eccentricity}) = \sqrt{(a^2 - c^2)/a^2} \approx 8.2 \times 10^{-2}. \quad (2.7)$$

Here, $g_{po} = g(0, \pi/2)$ is the surface gravity at the pole.

In ROPP, the parameters in Eqn (2.5) take the values

$$g_{eq} = 9.7803253359 \text{ ms}^{-2}; \quad k_s = 1.931853 \times 10^{-3}; \quad e = 0.081819.$$

Li and Götze ([7]) quote the following second order expansion of Eqn (2.5):

$$\text{Li and Götze: } g(0, \phi) = g_{eq}(1 + f^* \sin^2 \phi - 1/4 f_4 \sin^2 2\phi) \quad (2.8)$$

where

$$f^* = (g_{po} - g_{eq})/g_{eq} \approx 5.3 \times 10^{-3} \quad (2.9)$$

and

$$(1/4)f_4 = (f/8)(5m - f) \approx 5.9 \times 10^{-6}. \quad (2.10)$$

[Aside: Eqn (2.10) is a bit deus ex machina as it stands since it requires something like Eqn (2.19) below to get the rotation rate m into it. More consistent would be to say:

$$f^* = (1 + k_s)(1 + f) \approx 5.3 \times 10^{-3} \quad (2.11)$$

and

$$(1/4)f_4 = (f/4)(3f/2 + k_s) \approx 5.9 \times 10^{-6}. \quad (2.12)$$

]

Note that k_s (or g_{po}) in Somigliana's equation (Eqn (2.5)) must be specified directly: it is not derived from more elementary terms. Lambert ([4]) quotes a closed form expression for $g(0, \phi)$, due to Pizetti, which has the same form as Somigliana's equation, but with a derived value of (effectively) k_s :

$$\text{Pizetti: } g(0, \phi) = g_{eq}(1 + (mC - e^2) \sin^2 \phi) / \sqrt{1 - e^2 \sin^2 \phi}, \quad (2.13)$$

where

$$C = 5/2 - (13/7)\epsilon^2 \approx 2.5 \quad (2.14)$$

and

$$\epsilon(\text{second eccentricity}) = \sqrt{(a^2 - c^2)/c^2} \approx 8.2 \times 10^{-2}. \quad (2.15)$$

ROPP versions before 1.2 used an expression based on the Smithsonian Meteorological Tables (Lewis, 2007 [6], from a forerunner of [8]), which was a particular representation of Lambert's equation:

$$\text{SMT: } g(0, \phi) = \tilde{g}_{\text{eq}}(1 + \tilde{\beta} \sin^2 \phi - \tilde{\beta}_1 \sin^2 2\phi) \quad (2.16)$$

in which

$$\tilde{g}_{\text{eq}} = 9.780456 \text{ ms}^{-2}; \quad \tilde{\beta} = 5.2885 \times 10^{-3}; \quad \tilde{\beta}_1 = 5.9 \times 10^{-6}. \quad (2.17)$$

(The reader will notice these numbers are slightly different to those in Lambert's expression, Eqn (2.1).)

Finally, the surface gravity used in the *Invert* code is given by Lewis 2010 (pers. comm.):

$$\text{Invert: } g(0, \phi) = g_{\text{eq}}(1 + f_2 \sin^2 \phi - 1/4 f_4 \sin^2 2\phi) \quad (2.18)$$

where

$$\begin{aligned} g_{\text{eq}} &= GM/R_e^2 (1 - f + 3m/2 - 15mf/14) \\ f_2 &= -f + 5m/2 - 17mf/14 + 15m^2/4 \\ (1/4)f_4 &= (f/8)(5m - f) \end{aligned}$$

The *Invert* expression does not quite follow from Lambert's (Eqn (2.1)) or Pizetti's (Eqn (2.13)) formulas, but it does agree to first order in m and f . In fact, all three expressions imply that, to first order in these quantities, the ratio of the polar to the equatorial surface gravity is:

$$\text{Clairaut: } g_{\text{po}}/g_{\text{eq}} = 1 + (5/2)m - f \quad (2.19)$$

— a famous result due originally to Clairaut (eg see White et al 2008 [16]). Since $f \approx m \approx 1/300$, this means that surface gravity is about 0.5% larger at the poles than at the equator. Note further that m and f have opposing tendencies in Eqn (2.19): rotation makes gravity at the pole stronger than at the equator, while flattening makes it weaker. (This last result is discussed in more depth in the context of a simple toy model in the Appendix.)

Fig 2.1 compares expressions (2.1), (2.5), (2.8), (2.13), (2.16) and (2.18) for the surface gravity as a function of latitude. Lambert, Somigliana, Li and Götze, and Pizetti are effectively identical. The largest difference is between *Invert* and Somigliana, but even this incurs a fractional difference of less than 30 parts per million, which is probably negligible (see Sections 3 and 8).

Conclusion: No need to amend the surface gravity expression in ROPP.

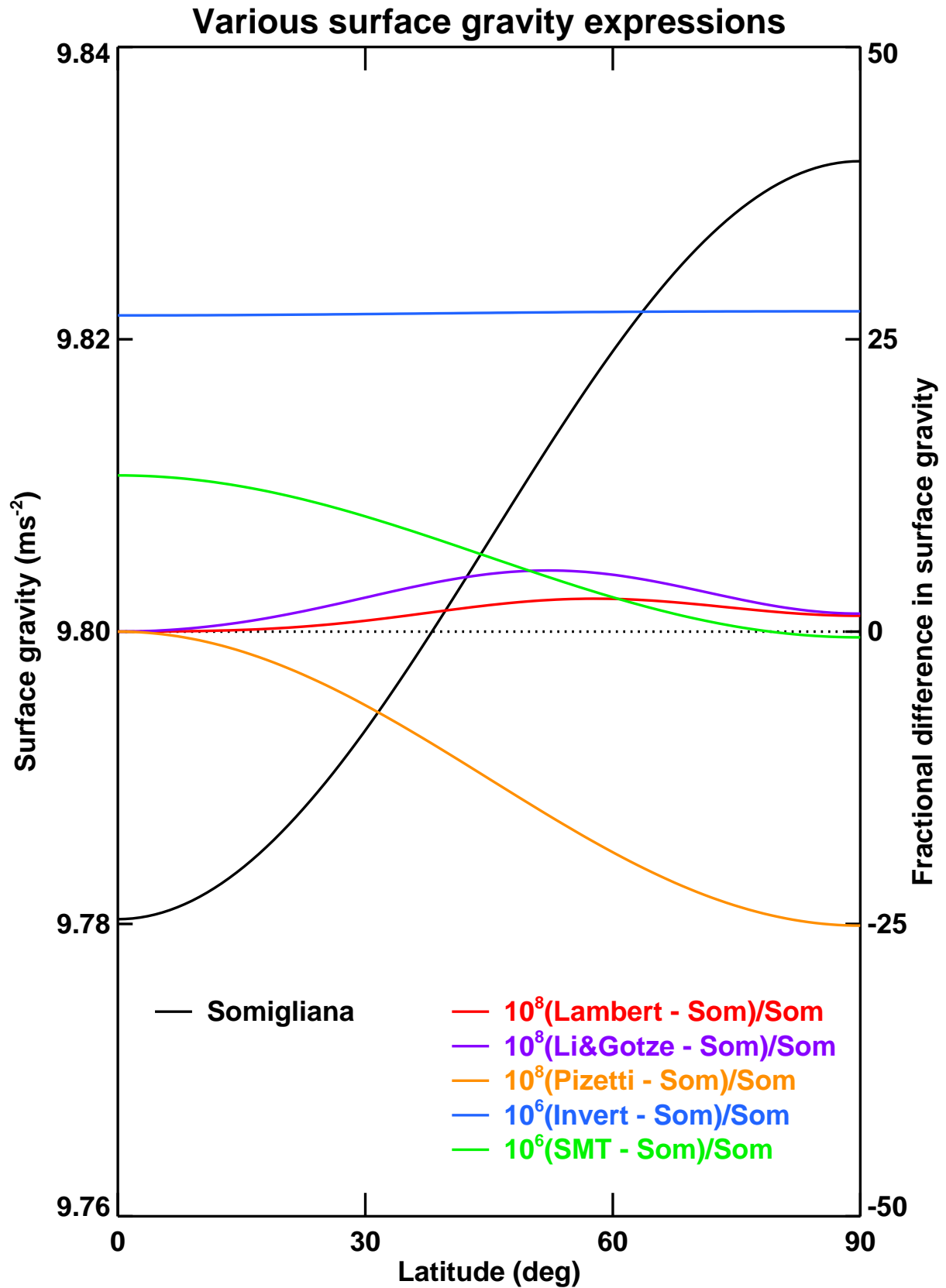


Figure 2.1: Latitudinal variation of surface gravity defined by Somigliana's equation, as used in ROPP, and fractional differences from it of alternative expressions. See text for details.

2.2 Variation with altitude

In a later paper, Lambert (1948 [5]) quotes the full International Gravity Formula for the variation of gravity with geodetic latitude and altitude normal to the ellipsoid. Since this does not seem to be widely known, we reproduce it in full:

$$\begin{aligned}
 \text{IGF: } g(h, \phi) = & g_{\text{eq}}(1 + \beta \sin^2 \phi - \beta_1 \sin^2 2\phi) \\
 & - 2g_{\text{eq}}(h/a)(1 + \alpha_0 + \alpha_1 \cos 2\phi + \alpha_2 \cos 4\phi) \\
 & + 3g_{\text{eq}}(h/a)^2(1 + \alpha_3 + \alpha_4 \cos 2\phi)
 \end{aligned} \tag{2.20}$$

where, in the notation of Section 2.1,

$$\begin{aligned}
 \alpha_0 &= (9/4)m - (1/2)f + f^2 - (173/112)mf \approx 6.1 \times 10^{-3} \\
 \alpha_1 &= (3/2)f - (5/4)m + (1/4)f^2 + (13/7)mf \approx 7.3 \times 10^{-4} \\
 \alpha_2 &= (1/4)f^2 - (5/16)mf \approx -8.2 \times 10^{-7} \\
 \alpha_3 &= -(2/3)f + (7/3)m \approx 5.9 \times 10^{-3} \\
 \alpha_4 &= 3f - (5/2)m \approx 1.4 \times 10^{-3}
 \end{aligned} \tag{2.21}$$

and a again is the semi-major axis of the ellipsoid of the Earth. The first line is just Eqn (2.1). Although Lambert is reticent about the origin of Eqn (2.20), the expression appears to derive from a complicated expansion of the geopotential in ellipsoidal co-ordinates — see, for example, Mahoney 2008 ([9]).

On a non-rotating, spherical planet, for which $m = f = 0$, α_0 – α_4 vanish and Eqn (2.20) reduces to the first two terms in the expansion of

$$g(h, \phi) = g(0, \phi) \left(\frac{a}{a+h} \right)^2 \tag{2.22}$$

as might be expected from the inverse square law of gravity.

In ROPP, the variation of gravity with altitude is handled analogously to Eqn (2.22), by means of the effective radius of the Earth, as will be discussed in the next Section.

Conclusion: The variation of gravity with height is not handled by the International Gravity Formula in ROPP.

3 Effective radius of Earth

In ROPP (and elsewhere) it is convenient to encode the variation of gravity with latitude and height in an analogous way to Eqn (2.22), by means of a fictitious, latitudinally varying, *effective radius* R_{eff} , by writing:

$$g(h, \phi) = g(0, \phi) \left(\frac{R_{\text{eff}}(\phi)}{R_{\text{eff}}(\phi) + h} \right)^2 \quad (3.1)$$

[Aside: there is no reason in general why g should fall off with height along a given latitude line exactly as $(R + h)^{-2}$. It isn't true, for instance, for the toy model discussed in the Appendix.]

If Eqn (3.1) is true, then $R_{\text{eff}}(\phi)$ is given by:

$$R_{\text{eff}}(\phi) = -2g(0, \phi) / g_h(0, \phi). \quad (3.2)$$

Note that the effective radius is a purely theoretical construct, invented to capture the variation of gravity with altitude, so that $g(h, \phi)$ can be written as Eqn (3.1). It bears no relation to the actual radius of the Earth. This becomes clear when Eqn (2.1) and Eqn (2.20) are substituted into Eqn (3.2): we obtain, to first order in m and f ,

$$\text{Lambert: } R_{\text{eff}}(\phi)/a = (1 + \beta \sin^2 \phi) / (1 + \alpha_0 + \alpha_1 - 2\alpha_1 \sin^2 \phi) \quad (3.3)$$

where a is again the semi-major axis of the spheroidal Earth.

Noting, as Mahoney (2008 [8]) does, that β and α_1 are positive, this means that $R_{\text{eff}}(\phi)$ *increases* towards the poles. (The equator-to-pole reduction in $g_h = \partial g / \partial h$ in the denominator of Eqn (3.2) is in fact about one third that of the increase of g in the numerator.) The fictitious nature of the effective radius is therefore clear — although perhaps not as well known as it should be.

[Aside: the effective radius of the simple model in the Appendix also increases with latitude.]

Mahoney quotes a corresponding expression to Eqn (3.3) using Somigliana's equation for gravity, Eqn (2.5). It has not been possible to reproduce this derivation. But the resulting effective radius, apparently given by

$$\text{Somigliana: } R_{\text{eff}}(\phi)/a = 1 / (1 + f + m - 2f \sin^2 \phi) \quad (3.4)$$

in which

$$a = 6378137.0 \text{ m}; \quad f = 0.003352811; \quad m = 0.003449787$$

is the one currently implemented in `ropp_utils/geodesy/r_eff.f90`.

ROPP versions before 1.2 used an expression for effective radius based on the Smithsonian Meteorological Tables (Lewis 2007 [6], from a forerunner of Mahoney 2008 [8]):

$$\text{SMT: } R_{\text{eff}}(\phi) = 2\tilde{g}_{\text{eq}}(1 + \tilde{\beta} \sin^2 \phi - \tilde{\beta}_1 \sin^2 2\phi) / (\gamma_0 + \gamma_1 \cos 2\phi + \gamma_2 \cos 4\phi) \quad (3.5)$$

in which \tilde{g}_{eq} , $\tilde{\beta}$ and $\tilde{\beta}_1$ are given by Eqn (2.17), and

$$\gamma_0 = 3.085462 \times 10^{-6} \text{ s}^{-2}; \quad \gamma_1 = 2.27 \times 10^{-9} \text{ s}^{-2}; \quad \gamma_2 = -2.0 \times 10^{-12} \text{ s}^{-2}.$$

For completeness, we record the effective radius used in the *Invert* code, which is given by Lewis 2010 (pers. comm.):

$$\text{Invert: } R_{\text{eff}}(\phi)/a = \left(\frac{g(0, \phi)}{g_{\text{eq}}} \right) (1 + f + m + (-3f + 5m/2) \sin^2 \phi)^{-1} \quad (3.6)$$

where $g(0, \phi)/g_{\text{eq}}$ is given by Eqn (2.18). To first order in m and f , Eqn (3.6) and Eqn (3.4) both imply

$$R_{\text{eff}}(\phi)/a \approx 1 - f - m + 2f \sin^2 \phi, \quad (3.7)$$

which is an increasing function of ϕ , as discussed above. (See the Appendix for further discussion.)

Fig 3.1 compares expressions (3.3), (3.4), (3.5) and (3.6). For comic relief, it also shows the actual radius of the Earth's ellipsoid as a function of latitude. The largest fractional difference in effective radii, between the expressions based on Somigliana's equation and the Smithsonian Tables, is about 65 parts per million. As will shortly be seen, this has a negligible impact in ROPP applications.

Conclusion: No need to amend the effective radius expression in ROPP.

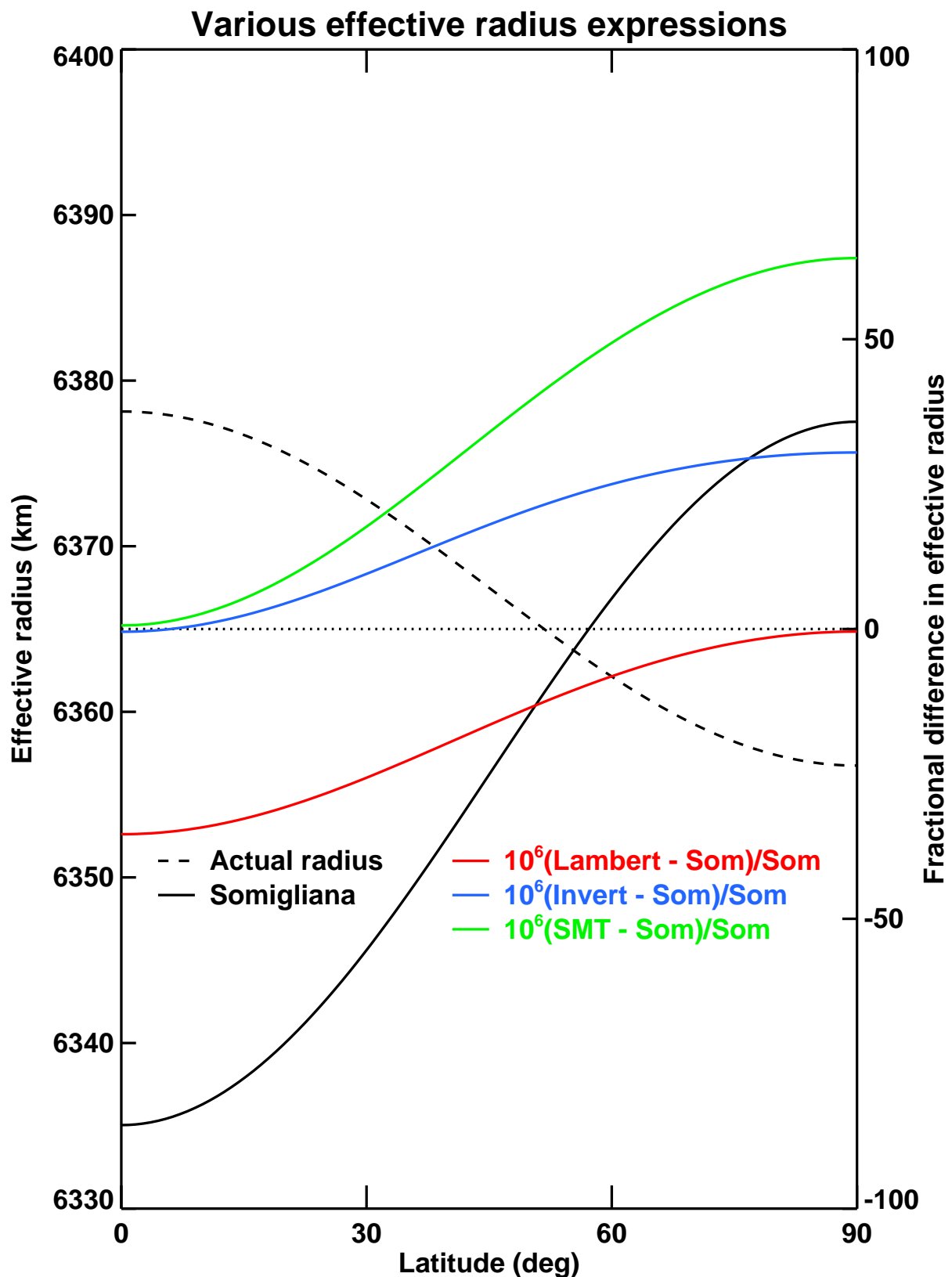


Figure 3.1: Latitudinal variation of effective radius defined by Somigliana's equation, as used in ROPP, and fractional differences with respect to it of alternative expressions. See text for details. Actual radius of Earth also shown.

4 Geopotential height

A key thing for radio occultation applications is the geopotential height Z at geometric height h , which is the (normalised) energy required to lift a unit mass air parcel from the surface geoid to that height:

$$Z(h, \phi) = g_{\text{ref}}^{-1} \int_0^h g(h', \phi) dh' \quad (4.1)$$

where g_{ref} is a normalising acceleration due to gravity.

Assuming an inverse square variation of gravity with height at each latitude, as in Eqn (3.1), Eqn (4.1) implies

$$Z(h, \phi) = \left(\frac{g(0, \phi)}{g_{\text{ref}}} \right) \left(\frac{R_{\text{eff}}(\phi)}{R_{\text{eff}}(\phi) + h} \right) h. \quad (4.2)$$

Since $R_{\text{eff}}(\phi) \gg h$, this implies

$$Z(h, \phi) \approx (g(0, \phi)/g_{\text{ref}}) h, \quad (4.3)$$

so that $Z(h, \phi)$ is almost independent of $R_{\text{eff}}(\phi)$. More precisely, Eqn (4.2) shows that (dropping arguments for clarity)

$$\frac{\delta Z}{Z} = \frac{\delta g}{g} + \left(\frac{h}{R_{\text{eff}} + h} \right) \frac{\delta R_{\text{eff}}}{R_{\text{eff}}}. \quad (4.4)$$

In ROPP work, $h \lesssim 60$ km, so $h/(R_{\text{eff}} + h) \lesssim 10^{-2}$, which means, as hinted above, that a given fractional difference in effective radius has a far smaller effect on geopotential height than a similar fractional change in surface gravity.

Fig 2.1 shows that $|\delta g/g| < 30 \times 10^{-6}$, and Fig 3.1 shows that $|\delta R_{\text{eff}}/R_{\text{eff}}| < 65 \times 10^{-6}$. Overall, then, the fractional difference in geopotential height is dominated by the difference in surface gravities. This is borne out by Fig 4.1, which shows the differences in geopotential heights calculated using formulas for g and R_{eff} calculated using Somigliana's formulas, Lambert's formulas, the *Invert* code and the SMT tables. It is clear that $\delta Z/Z$ in Fig 4.1 largely reflects $\delta g/g$ in Fig 2.1. The largest difference is between the *Invert* code and Somigliana's expression, as would be expected from Fig 2.1 and Eqn (4.4), but even this is only about 30 parts per million, which equates to 2.4 m at 80 km, and which is probably negligible. It corresponds to a temperature difference of about 0.012 K at a typical mesospheric lapse rate of 5 K/km.

Similarly, for the inverse relation between geometric height and geopotential height, also needed in ROPP,

$$h(Z, \phi) = \left(\frac{R_{\text{eff}}(\phi)}{(g(0, \phi)/g_{\text{ref}})R_{\text{eff}}(\phi) - Z} \right) Z, \quad (4.5)$$

we find, approximately,

$$\frac{\delta h}{h} = -\frac{\delta g}{g} - \left(\frac{h}{R_{\text{eff}}} \right) \frac{\delta R_{\text{eff}}}{R_{\text{eff}}}. \quad (4.6)$$

Since $h \ll R_{\text{eff}}$, the same weak dependence on $R_{\text{eff}}(\phi)$ results.

[Aside: Lewis 2007 ([6]) found changes in $Z \lesssim 1$ m between the earlier SMT expressions for g and R_{eff} , and the later ones based on Somigliana's equation, when the difference in R_{eff} was $\lesssim 300$ m. As above, is clear that in this case the majority of the difference was coming from $\delta g/g$.]

Conclusion: No need to amend the surface gravity or effective radius expressions in ROPP.

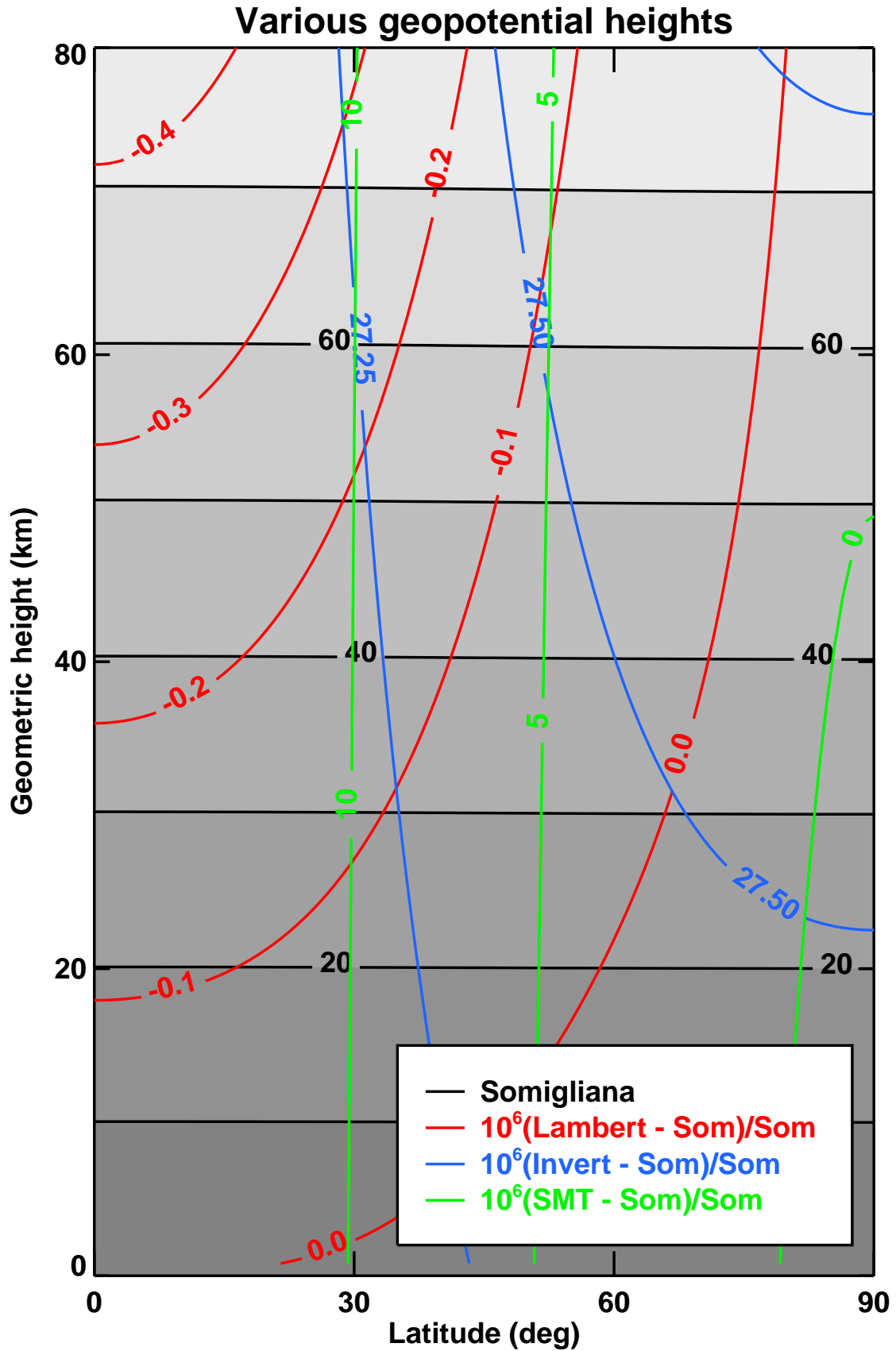


Figure 4.1: Latitudinal and vertical variation of geopotential height defined by Somigliana's equation, as used in ROPP, and fractional differences from it of alternative expressions. See text for details.

5 Radius of curvature

Sections 2, 3 and 4 have been concerned with the mass and rotation of the Earth, and their influence on its gravitational field. The radius of curvature is a more geometrical idea, associated, in the context of radio occultation, with the curvature of the Earth in the vicinity of the tangent point. The local centre of curvature, thus defined, is the natural place to site the origin of the co-ordinate system used to calculate the ray path, bending angle, and so forth.

In this co-ordinate system, the local shape of the geoid is approximated by a circle with the same curvature as the intersection of the (assumed) ellipsoidal mean sea level geoid with the plane of the occultation (Rodgers, 2000, pp 148-149 [13]). The resulting radius of curvature is very different from the actual local radius of the Earth: greater at the pole, and (except for strictly E-W occultations) smaller at the equator. Rodgers quotes the formulas:

$$R_{NS}(\phi) = a^2 c^2 (a^2 \cos^2 \phi + c^2 \sin^2 \phi)^{-3/2} \quad (5.1)$$

$$R_{EW}(\phi) = a^2 (a^2 \cos^2 \phi + c^2 \sin^2 \phi)^{-1/2} \quad (5.2)$$

$$R_c(\phi, \alpha)^{-1} = R_{NS}(\phi)^{-1} \cos^2 \alpha + R_{EW}(\phi)^{-1} \sin^2 \alpha \quad (5.3)$$

in which R_{NS} and R_{EW} are respectively the “meridional” and “normal” radii of curvature at geodetic latitude ϕ , and R_c is the radius of curvature in the plane at azimuth (ie bearing with respect to true north) α .

In ROPP, Eqn (5.3) is evaluated in `ropp_utils/coordinates/curvature.f90`¹.

$R_c(\phi, \alpha)$ is plotted in Fig 5.1. Note the 42 km difference in radius of curvature between E-W and N-S occultations on the equator. There is of course no variation in radius of curvature at the pole.

To first order in the small quantity e^2 we find

$$R_{NS}(\phi)/a \approx 1 + 1/2 e^2 (3 \sin^2 \phi - 2) \quad (5.4)$$

$$R_{EW}(\phi)/a \approx 1 + 1/2 e^2 \sin^2 \phi \quad (5.5)$$

$$R_c(\phi, \alpha)/a \approx 1 + 1/2 e^2 (\sin^2 \phi - 2 \cos^2 \phi \cos^2 \alpha) \quad (5.6)$$

The maximum $|\partial R_c / \partial \alpha|$ occurs on the equator when $\alpha = \pm\pi/4, \pm 3\pi/4$, and equals $ae^2 = 730$ m/deg. The maximum $|\partial R_c / \partial \phi|$ occurs when $\alpha = 0, \phi = \pm\pi/4$, and equals $3/2ae^2 = 1100$ m/deg. *Both of these are rather large sensitivities, and highlight the need for accurate estimation of latitude and azimuth to avoid significant error in the calculation of the radius of curvature.*

The arithmetic average of R_c over azimuth, assuming all azimuths α to be equally likely, is:

$$\langle R_c \rangle(\phi)/a = \sqrt{R_{NS}(\phi)R_{EW}(\phi)}/a \quad (5.7)$$

$$\approx 1 + e^2 \sin^2 \phi - 1/2 e^2 \quad (5.8)$$

which shows that the average radius of curvature increases with latitude.

Comparison of Eqn (5.8) with Eqn (3.7), and using $m \approx f \approx 1/2e^2$, shows that, excitingly, the mean radius of curvature exceeds the effective radius of the Earth by a constant offset of $1/2ae^2 \approx 21$ km. (Recall that neither bears much similarity to the actual radius of the Earth.)

¹The present formulation in ROPP contains some slight numerical infelicities which will be put right at ROPP8.0.

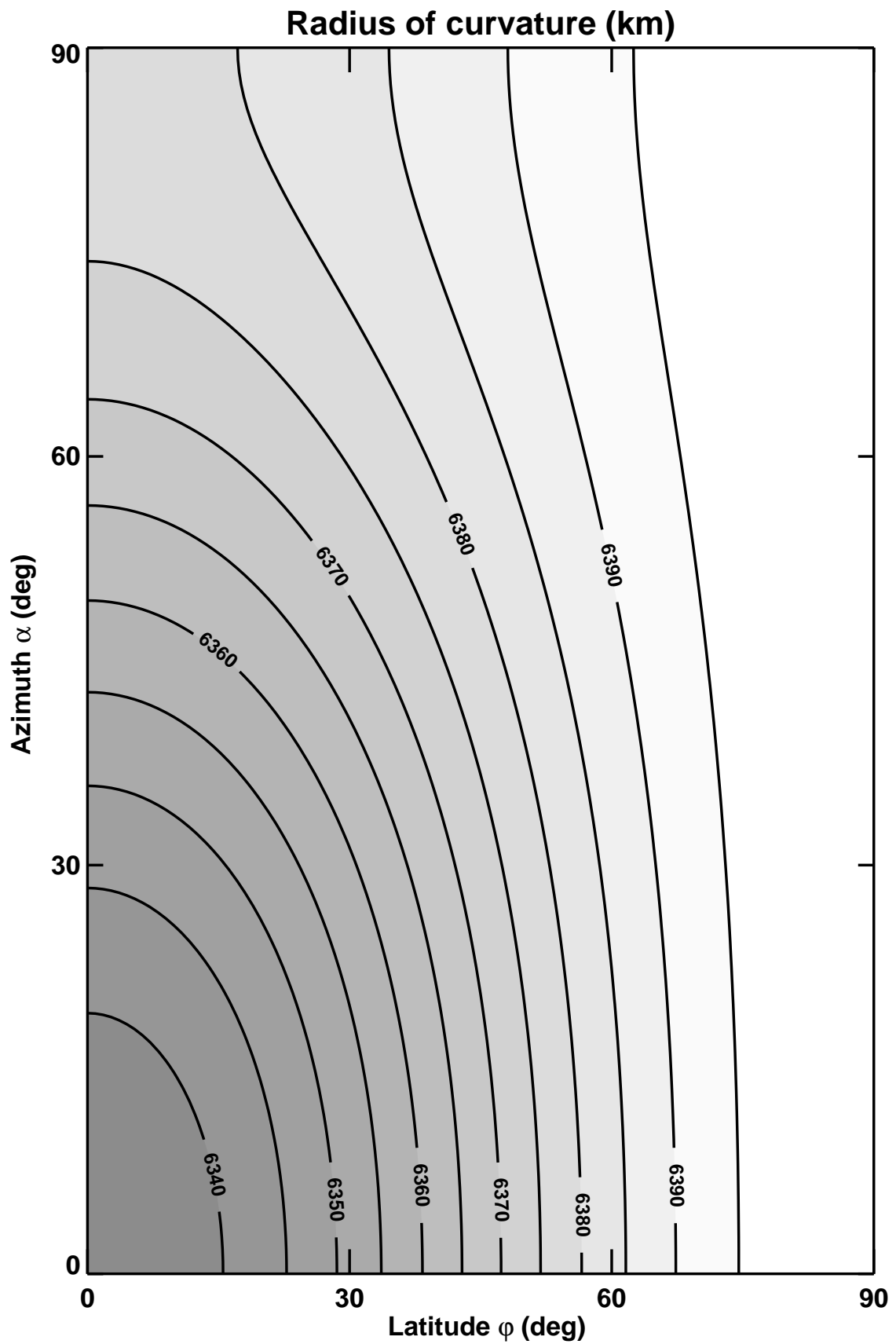


Figure 5.1: Latitudinal and azimuthal variation of Earth's radius of curvature.

R_{NS} , R_{EW} and $\langle R_c \rangle$ are plotted as functions of latitude in Fig 5.2. The actual radius of the Earth's ellipsoid as a function of latitude, which is given to first order in e^2 by

$$R_{\text{Earth}}(\phi)/a \approx 1 - 1/2e^2 \sin^2 \phi, \quad (5.9)$$

is also plotted. Eqns (5.8) and (5.9), and consideration of the angle between the normal and radial vectors on the spheroidal Earth, imply that the (azimuthally averaged) centre of curvature is displaced from the centre of the Earth by an amount which, it turns out, varies from 21 km at the equator to 42 km at the pole. In fact, to first order in e^2 the magnitude of this displacement can be shown to be given by

$$|R_{\text{Earth}}\hat{\mathbf{r}} - \langle R_c \rangle\hat{\mathbf{n}}| \approx 1/2ae^2 \sqrt{1 - 2\sin^2 \phi + 5\sin^4 \phi}, \quad (5.10)$$

(where $\hat{\mathbf{r}}$ is the unit radial vector and $\hat{\mathbf{n}}$ is the unit normal vector). This quantity is also plotted in Fig 5.2. For the record, the corresponding displacements for E-W and N-S occultations are respectively given by

$$|R_{\text{Earth}}\hat{\mathbf{r}} - R_{EW}\hat{\mathbf{n}}| \approx ae^2 |\sin \phi| \quad (5.11)$$

$$|R_{\text{Earth}}\hat{\mathbf{r}} - R_{NS}\hat{\mathbf{n}}| \approx ae^2 \sqrt{1 - 3\sin^2 \phi + 3\sin^4 \phi}. \quad (5.12)$$

All of these scale with the equatorial excess, $1/2ae^2 \approx 21$ km. Correctly accounting for the oblateness of the Earth is crucial for the correct interpretation of radio occultation measurements (Kursinski et al 2000 [3], Syndergaard 1998 [15]).

Conclusion: No reason to amend the curvature calculations in ROPP.

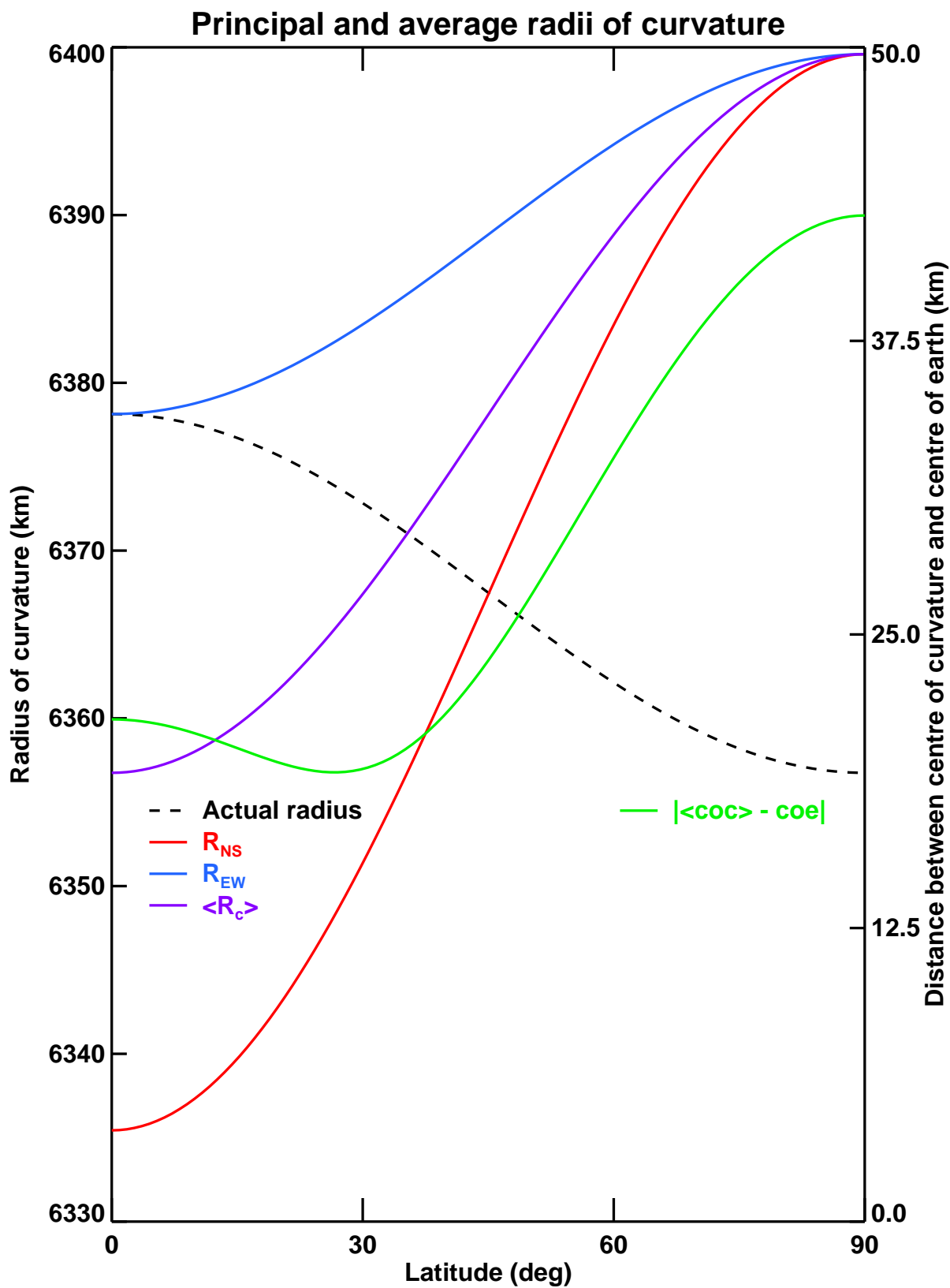


Figure 5.2: Latitudinal variation of various terrestrial radii of curvature, and of distance between average centre of curvature and centre of Earth.

6 Undulation

Thus far, this report has assumed that the geoid — that is, the equipotential surface that best fits the Earth’s mean sea level — is described as an ellipsoid: usually (and certainly in ROPP) the WGS84 ellipsoid (NGIA 2010 [11]). This is not quite true: the two surfaces differ because of localised variations in the Earth’s gravitational field. The difference between the height of the geoid and the height of the ellipsoid is known as the *undulation*, u .

In this sense the undulation provides a connection between the physical and the mathematical aspects of geodesy in radio occultation: the geoid and the ellipsoid.

The undulation of the EGM96 geoid model (NASA 2004 [10]), evaluated on a $1/4^\circ \times 1/4^\circ$ grid, is plotted in the top panel of Fig 6.1, and the magnitude of its gradient is plotted in the bottom panel (note the logarithmic colour scale). The range of the undulation is no more than about ± 100 m, and appears relatively smooth. The highest gradients follow mountain ranges and undersea ridges. Around half the points have undulation gradients greater than about 2×10^{-5} m/m in magnitude. Over a 400 km drift in the tangent point during an occultation, this could accumulate to a change in undulation of about 8 m, which is unlikely to be significant. Presently in ROPP, therefore, a fixed undulation is assumed throughout the occultation.

In most ROPP applications the undulation is provided by the data provider as a single number. But in the `ropp_pp` module, which generates bending angles and refractivities from level 1a excess phase data, the (single) undulation at the nominal tangent point location is calculated from the (order and degree 360) spherical harmonic expansion of the EGM96 geoid provided by NASA (2004 [10]). The highest order spherical harmonic in this expansion has a wavelength of $1^\circ \sim 110$ km along the equator, which should be just enough to resolve undulations on 400 km scales. If, however, a better resolved undulation were desired at some point in the future, then it may become necessary to use a higher order expansion, such as EGM2008 ([11]), which is of order and degree 2159, and which has a minimum wavelength of about 18 km.

[Aside: In `ropp_pp`, why not simply store the 2D field shown in Fig 6.1 and interpolate from that? See a forthcoming RSR for further discussion.]

The undulation is needed to convert between impact parameters $n(r)r$, which involve distances r from the centre of curvature (Section 5), and geometric heights h , which are measured with respect to the geoid, thus:

$$r = h + u + R_c. \tag{6.1}$$

The geometric heights h are converted to and from geopotential heights Z , on which model variables are defined, by means of Eqns (4.2) and (4.5). These equations, in which $g_{\text{ref}} = 9.80665 \text{ ms}^{-2}$, are the ones currently implemented in `ropp_utils/geodesy/geometric2geopotential.f90` and `ropp_utils/geodesy/geopotential2geometric.f90` respectively.

Conclusion: Until undulations that vary through the occultation are required, there is no need to improve the treatment of undulation in ROPP.

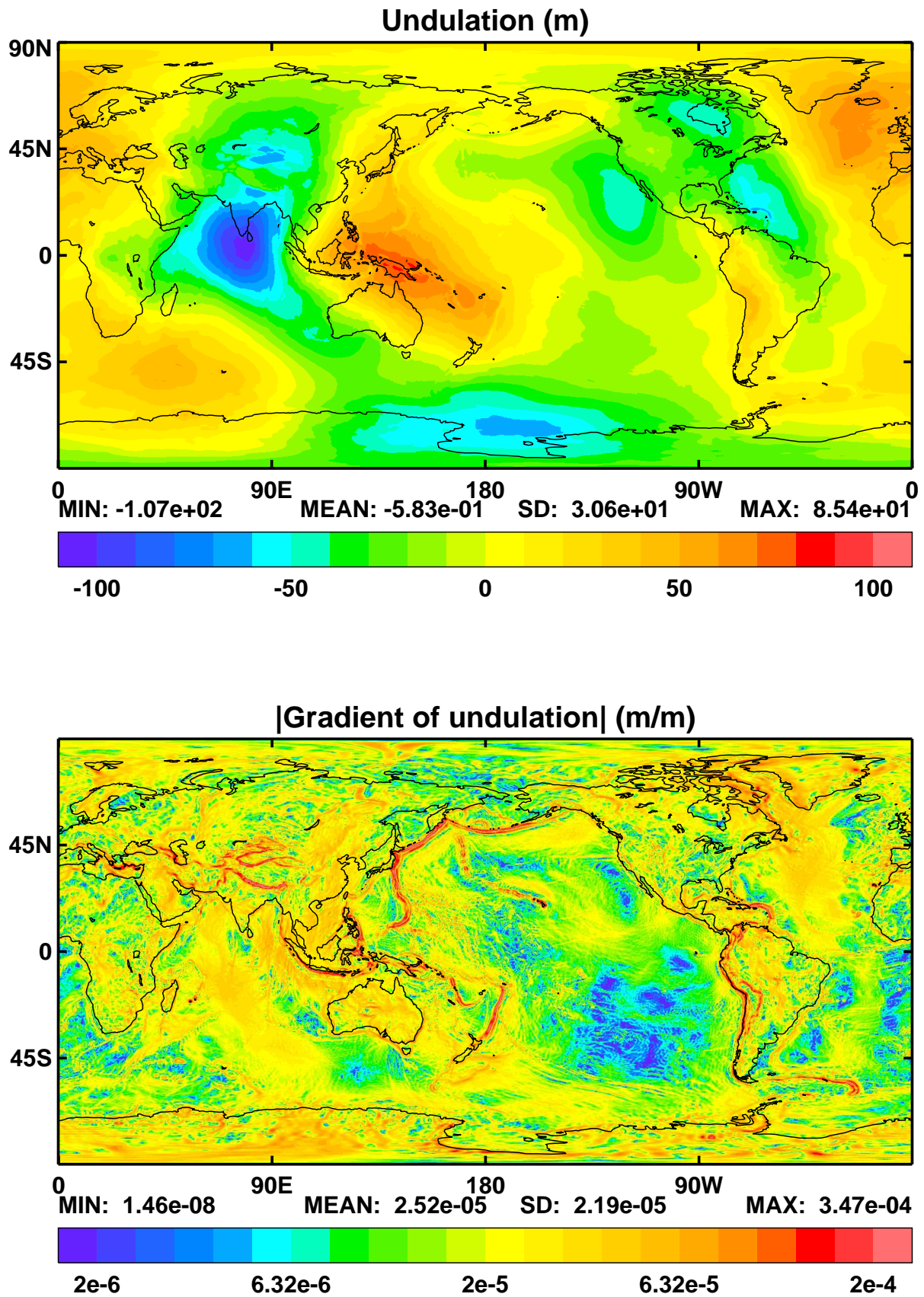


Figure 6.1: Spatial variation of: (top) undulation; and (bottom) magnitude of gradient of undulation. Data from EGM96 ([11]).

7 Response to ROPP2.0 beta reviewer's comments

The ROPP2.0 beta reviewer (GRAS SAF 2008 [1]) made two specific comments on the geodesy calculations in ROPP.

Geometric vs geopotential transformations: *Several details were found not to be of sufficient accuracy. The expressions used conform to estimations that are standard in meteorological contexts. However, they are less accurate than the GPSRO technology is, and thus will become the limiting factor for the data. The reviewer considers this as “correct” in the sense that it conforms to standard practice. However this should be addressed in future ROPP versions.*

(Much) later contact with the reviewer revealed his concern that . . .

. . . the geopotential/geometric transformation did not account for the variation of gravity with latitude and altitude. This has to be considered in the hydrostatic equation. Either using a constant value for the acceleration of gravity ($g=g_0$), and remembering that the values obtained are geopotential altitudes, or using a variable gravity field ($g=g(\text{lat},h)$) according to some suitable model (I presume that the ellipsoidal WGS-84 is enough) and obtaining geometric altitudes.

This may have been modified since then.

It has indeed: as discussed in Section 2 a full expression for $g(h, \phi)$ based on Somigliana's equation is now used in ROPP (`ropp_utils/geodesy/gravity.f90`). The discussions in Sections 2–4, and the sensitivity studies to be considered in the next Section, suggest that any quibbles about the preferred form of $g(h, \phi)$ are unlikely to have a large practical impact in ROPP.

Earth radius: *The quantity estimated (Somigliana) is not the radius of curvature. It is not an accurate estimation of the radius of curvature (which depends not only on latitude, but also on the azimuth). It is not more accurate for the estimation of the geopotential than a fixed average radius. Instead, it is much more computationally expensive. The error is comparatively small in the way and context that this quantity is used in this release. However, it could lead to very substantial errors if this quantity was used in other contexts within GPSRO applications where the Earth radius is also needed. This should be addressed as future releases of ROPP may very likely require this quantity for other purposes.*

The distinction between effective radius and radius of curvature has been discussed extensively in this report. There appears to be no confusion in ROPP2.0 between the two: where needed, the radius of curvature is read from input files. (The `ropp_pp` module was very rudimentary at ROPP2.0, and contained none of the routines that, in later releases, calculate the radius of curvature using Eqn (5.3).) We agree with the reviewer that a varying R_{eff} is not much more accurate for calculations of geopotential than a constant one. (See Section 8.2 for evidence in support of this.) But a difference between R_{eff} and R_c of 21 km (see the discussion after Eqn (5.8)) would, according to Eqn (4.4), result

in a fractional difference in geopotential height of 30 parts per million at 60 km. Coincidentally, this matches the contribution to $\delta Z/Z$ arising from the maximum uncertainty in $\delta g/g$ shown in Fig 2.1, as discussed, and dismissed, in Section 3. For the same reasons, then, a constant effective radius would likely be sufficiently accurate for ROPP. Equally, a latitudinally varying effective radius is not more *inaccurate*. We dispute that using Eqn (3.4) is “much more computationally expensive” than using a constant R_{eff} : both take a negligible fraction of the total CPU time of any ROPP calculation. In view of the costly need to revalidate ROPP following revision of the effective radius, we consider it acceptable to leave it alone.

The reviewer’s last two sentences refer to the risks of mistaking R_{eff} for R_c . We agree that this could potentially be a problem, but as pointed out above, the two quantities are now calculated independently and correctly throughout ROPP. In fact, the effective radius is not part of the `ROpprof` structure in ROPP, is never output from ROPP, and should therefore never be confused with the radius of curvature. (The difference is stressed in the ROPP User Guides.) However, as the reviewer pointed out later:

The radius of curvature in the sense of divergence of the gravity field (Somigliana) or the osculating circle to the Earth (azimuth-dependent) are indeed different, but the Somigliana value was being used for the osculating circle. This was incorrect, and the team answered to the report that this was too small to be of concern. This depends on what the users do with these values, so I was recommending that they were corrected.

*Both may now be evaluated in ROPP, but **the Somigliana value is still used in distributed (bufr) data**, in the “radius of curvature” placeholder, as I have recently verified.*

It is my understanding that this placeholder is intended to set a geometric reference point for the impact parameter values, and expresses the distance to the center of curvature that was used in the doppler-to-bending transformation (level 1a to level 1b). It should therefore be the radius of the osculating circle. I suspect that the doppler-to-bending was performed with respect to an incorrect center of curvature.

We confirmed that the radius of curvature appearing in the BUFR files produced by the ROM SAF was inconsistent with that calculated from the latitude and azimuth in the file, although it was not in fact equal to the (Somigliana) effective radius. Further investigation revealed the cause to be an inexact azimuth: the radius of curvature was correct. The inconsistency arose because the level 1a data provider, EUMETSAT, supplied a (nominal) latitude and radius of curvature for each profile, but not an azimuth. The BUFR files were generated by DMI, who provided an estimated azimuth based on extrapolation from the top of the profile. Although the difference between this and the true azimuth was usually less than one degree, the discussion after Eqn (5.6) shows that this could be large enough to cause the ~ 500 m difference in the radius of curvature found by the reviewer when he calculated the radius of curvature from the data in the file. EUMETSAT now provide the actual azimuth that was used in the processing to bending angle, and DMI will be distributing it in the BUFR files in due course. When this azimuth is used in `ropp_utils/coordinates/curvature.f90`, the resulting radius of curvature matches the one in the file. ROPP is therefore calculating the radius of curvature correctly.

(In the course of these later investigations the reviewer discovered some numerical unpleasantness in the ROPP routines, namely: indeterminacy at the pole and floating point overflow if evaluated at single precision. These minor failings will be put right at the next release of ROPP.)

Conclusion: No reason to amend ROPP’s effective radius or radius of curvature routines.

8 Sensitivity studies

We are not currently in a position to say which, if any, of the geodesy expressions described in Sections 2, 3 and 4 are ‘correct’, or even which is best. All we can ask is that the differences between them have small enough impacts in radio occultation applications that the question can be deferred. We have therefore carried out a series of (strong) sensitivity tests to see if the assertions made in Section 7 are true in practice.

8.1 Sensitivity to surface gravity

We examine the impact of setting $g(0, \phi)$ equal to a constant value.

The control experiment uses the standard ROPP expression for surface gravity, Eqn (2.5):

$$\text{control: } g(0, \phi)/g_{\text{eq}} = (1 + k_s \sin^2 \phi) / \sqrt{1 - e^2 \sin^2 \phi}. \quad (8.1)$$

In the test experiment this is replaced by its average over all latitudes:

$$\text{test: } \langle g(0, \phi) \rangle / g_{\text{eq}} \approx (1 + 1/2k_s + 1/4e^2) \approx 1.0026. \quad (8.2)$$

The difference in $g(0, \phi)$ between Eqns (8.1) and (8.2) is around 0.25% at most.

The top two panels of Fig 8.1 show the fractional change in refractivity and bending angle that arise when 625 ECMWF background profiles, co-located with 625 (ie, one assimilation cycle of) GRAS bending angle profiles, are passed through the test and control one-dimensional forward models in `ropp_fm`. The changes in refractivity, and consequently bending angle, are implicit: they arise because the refractivity altitude h has altered in accordance with Eqn (4.6) in Section 4. Fig 8.1 therefore shows the difference in refractivity that arises when test results are interpolated to the control altitudes before differencing. This effective change in refractivity affects the bending angle as shown.

The mean fractional differences in both fields has a ‘shoulder’ at around 15 km, which is unexplained. It may be associated with the tropopause. Below this height, fractional differences in refractivity and bending angle are very small; above it, they are about 0.2% smaller in the test. This might be expected, given that the change in surface gravity between test and control (ie, between Eqn (8.2) and Eqn (8.1)) is also around 0.25% at most (see Fig 2.1). Noting, from the same figure, that the differences between the actual possible expressions for surface gravity are much less than 0.01%, this suggests very little sensitivity to realistic uncertainty in surface gravity.

The bottom two panels of Fig 8.1 show the fractional change in temperature and humidity that arise when the same 625 background and GRAS bending angle profiles are passed through the test and control versions of the retrieval tools in `ropp_1dvar`. Temperature retrievals have insignificant differences throughout. There is more difference in the specific humidities, whose averages differ by

as much as 1%. It is not unusual for retrieved specific humidities to be more sensitive to details of the retrieval scheme than the temperatures¹. Despite this, the fractional differences in q are comparable to the fractional differences in g that caused them, and so we again conclude that there is likely to be little sensitivity in practice to the realistic uncertainty in surface gravity. This lends confidence to our response to the ROPP2.0 beta reviewer's first comment.

Conclusion: ROPP is largely insensitive to the expression for the surface gravity of the Earth.

¹For example, whether `minROPP` or `LevMarq` are used in the minimiser. (`minROPP` is used here.)

Sensitivity to making surface gravity constant

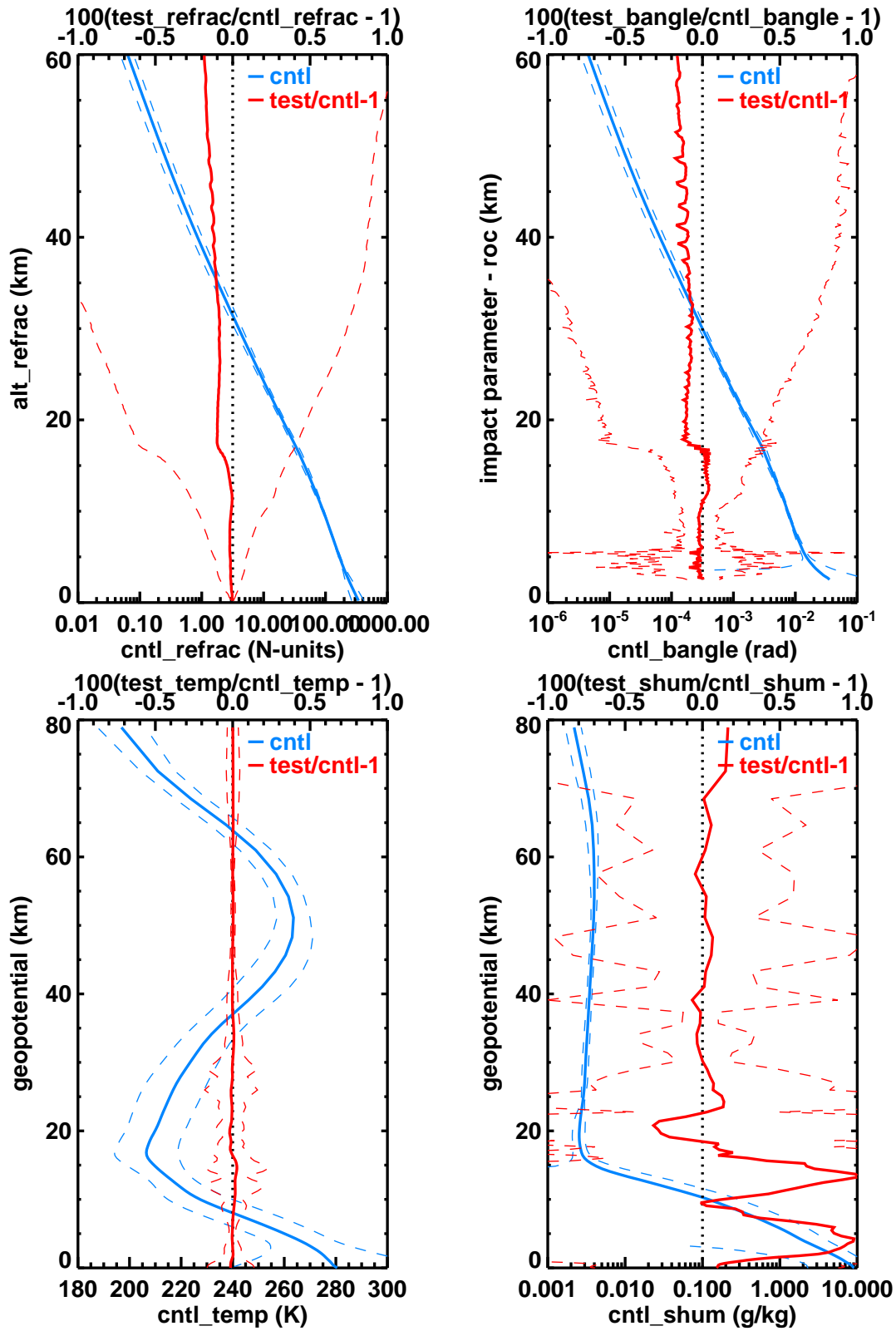


Figure 8.1: Sensitivity of (top) `ropp_fm` and (bottom) `ropp_1dvar` routines to the surface gravity. 'cntl' = Somigliana's expression Eqn (8.1); 'test' = constant value Eqn (8.2). Solid curve = mean, dashed curves = mean \pm one standard deviation.

8.2 Sensitivity to effective radius

We examine the impact of setting the effective radius $R_{\text{eff}}(\phi)$ equal to a constant value.

The control experiment uses the standard ROPP expression for effective radius, Eqn (3.4):

$$\text{control: } R_{\text{eff}}(\phi)/a = 1/(1 + f + m - 2f \sin^2 \phi). \quad (8.3)$$

In the test experiment this is replaced by its average over all latitudes:

$$\text{test: } \langle R_{\text{eff}} \rangle / a = ((1 + m)^2 - f^2)^{-1/2} \approx 0.9966. \quad (8.4)$$

The difference in R_{eff} between Eqns (8.3) and (8.4) is around 0.4% at most.

The test design and data are the same as described in Section 8.1. Fig 8.2 shows the analogous results, but with the fractional changes plotted on an ten-fold expanded scale. Typical differences in the two experiments are much less than 0.01%, except (as before) for specific humidity retrievals, which differ by as much as 0.1% on average. Thus, as expected from the discussion in Section 4, a change in $\delta g/g$ has a larger effect than a comparable change in $\delta R_{\text{eff}}/R_{\text{eff}}$. And noting from Fig 3.1 that the differences between the various expressions for R_{eff} are less than 0.01%, this suggests very little sensitivity to realistic uncertainty in effective radius. This too lends confidence to our response to the ROPP2.0 beta reviewer's first comment.

Conclusion: ROPP is very insensitive to the expression for the effective radius of the Earth.

Sensitivity to making effective radius constant

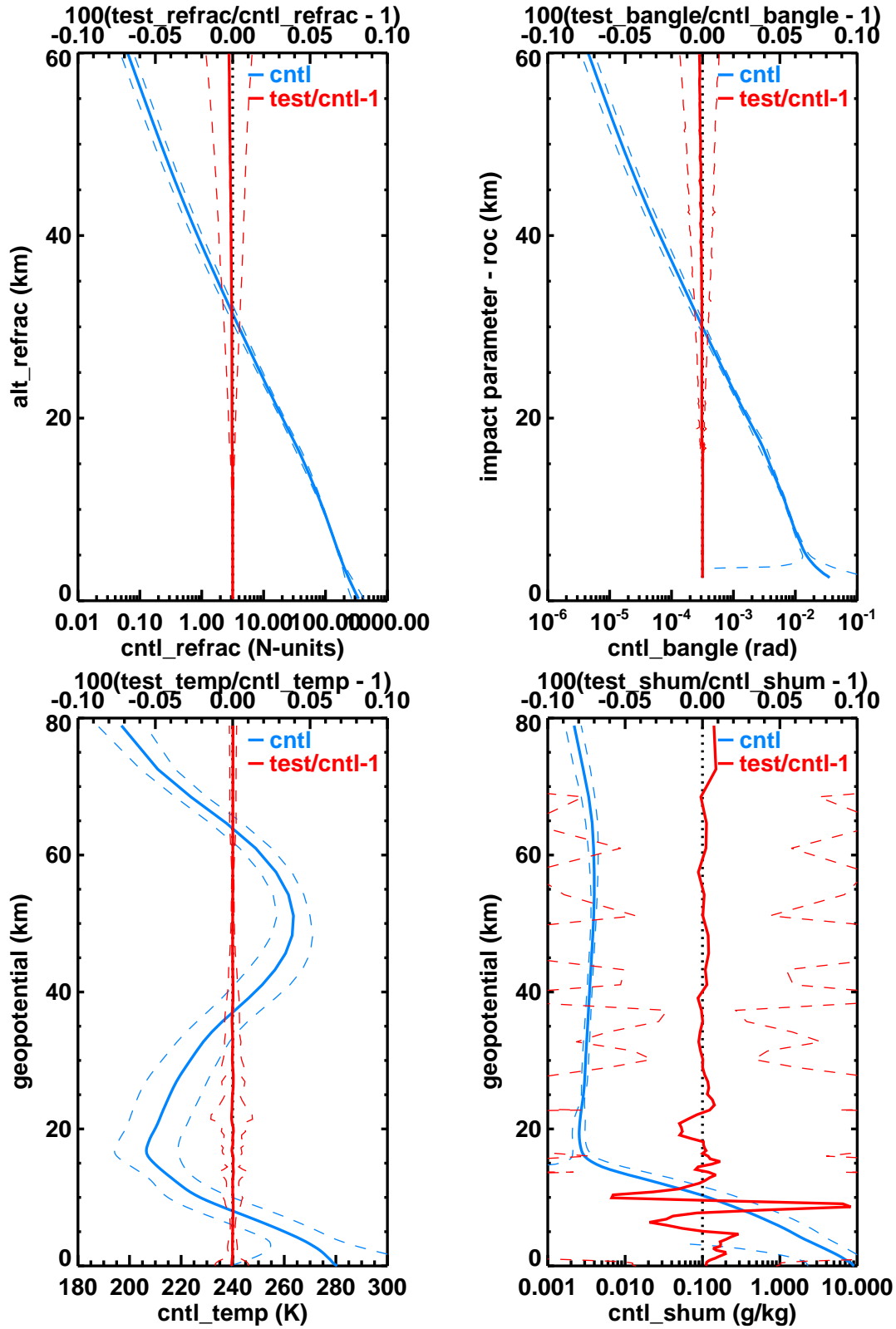


Figure 8.2: Sensitivity of (top) `ropp_fm` and (bottom) `ropp_1dvar` routines to the effective radius. 'cntl' = Somigliana's expression Eqn (8.3); 'test' = constant value Eqn (8.4). Solid curve = mean, dashed curves = mean \pm one standard deviation.

8.3 Sensitivity to radius of curvature

We next examine the impact of setting the azimuthally averaged radius of curvature $\langle R_c \rangle(\phi)$ equal to a constant value.

The control experiment uses the standard ROPP expression for radius of curvature, Eqn (5.8):

$$\text{control: } \langle R_c \rangle(\phi)/a \approx 1 - e^2 \cos^2 \phi + 1/2e^2. \quad (8.5)$$

In the test experiment this is replaced by its further average over all latitudes:

$$\text{test: } \langle \langle R_c \rangle \rangle / a \approx 1. \quad (8.6)$$

The difference in $\langle R_c \rangle(\phi)$ between Eqns (8.5) and (8.6) is around 0.4% at most.

The *calculation* of R_c has no impact on `ropp_fm` or `ropp_ldvar`, but its value, which appears as an input parameter to these modules, affects the forward modelled bending angles, through a shift of the ‘ r ’ element of the impact parameter $n(r)r$. More interesting is the sensitivity to R_c in the `ropp_pp` module – specifically, the effect on the bending angle and refractivity profile calculated from L1 and L2 excess phase signals.

The top two panels of Fig 8.3 show the sensitivity to setting $\langle R_c \rangle$ constant on bending angles (derived by wave optics) and refractivities (derived by inverse Abel transform) when 24 COSMIC profiles processed by tools in `ropp_pp`. The bending angles differ by over 5% at the bottom of the profile and up to about 0.5% before they get very noisy above about 70 km. The refractivities show a more consistent bias above about 50 km. (Presumably they are smoother because they are derived by integrating the bending angles upwards.) The bottom two panels show the impact on dry temperature and pressure, as derived by hydrostatic integration of the refractivity, when the air is assumed to be completely dry. There are differences in the mean temperature of up to 0.5%, which amounts to around 1–2 K. Similarly, the dry pressure differs by over 1% at height. These differences are probably too large to be ignored. Hence we conclude that proper account of the variation in radius of curvature needs to be retained in ROPP. This tallies with the ROPP2.0 beta reviewer’s second point.

Conclusion: ROPP is sensitive to the expression for the radius of curvature at the tangent point.

Sensitivity to making radius of curvature constant

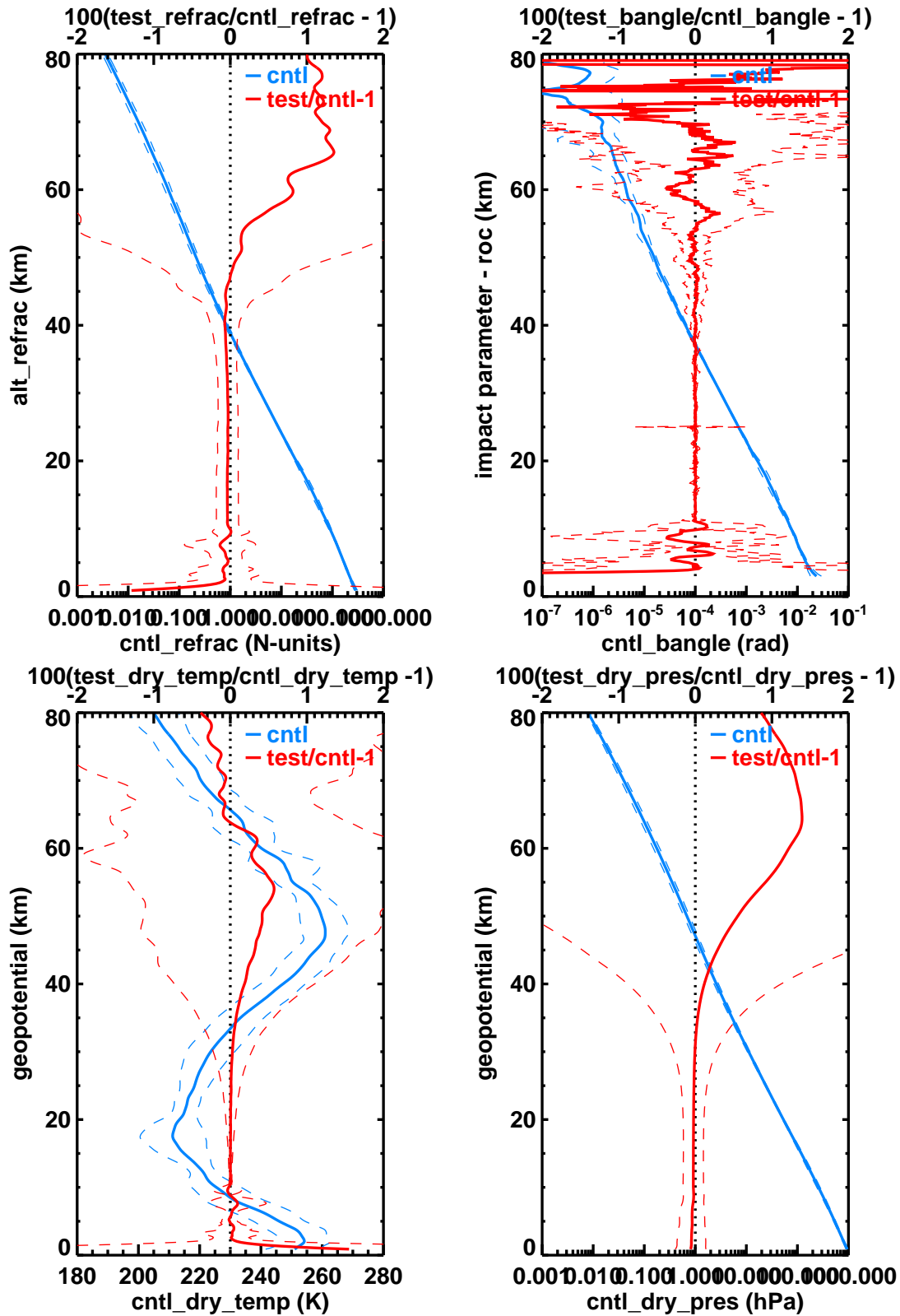


Figure 8.3: Sensitivity of `ropp_pp` routines to the radius of curvature. 'cntl' = Rodgers' expression Eqn (8.5); 'test' = constant value Eqn (8.6). Solid curve = mean, dashed curves = mean \pm one standard deviation.

8.4 Sensitivity to undulation

Finally, we examine the impact of setting the undulation u equal to a constant value.

The control experiment uses the standard ROPP expression for the relation between the radius and the geometric height Eqn (6.1):

$$\text{control: } r = h + R_c + u. \quad (8.7)$$

In the test experiment the undulation component of this expression is replaced by zero:

$$\text{test: } r = h + R_c. \quad (8.8)$$

(The mean undulation is in fact about -60 cm — see Fig 6.1 in Section 6.) The difference in u between Eqns (8.7) and (8.8) is around 100 m at most.

The results of passing test and control through the `ropp_fm` operators are shown in the top two panels of Fig 8.4. The change in undulation implies an implicit change in bending angles, but has no effect on refractivities (or their altitudes). The bending angles differ by up to 0.5% at the bottom, with large variation. This change in bending angles leads to a very small change in the retrieved temperatures, and a maximum difference of perhaps 0.25% in the specific humidities. These are not very great sensitivities.

(Regrettably the COSMIC profiles used in the previous `ropp_pp` sensitivity tests have missing undulations, which prevents them from being used in this study.)

Conclusion: ROPP is weakly sensitive to the undulation.

Sensitivity to making undulation zero

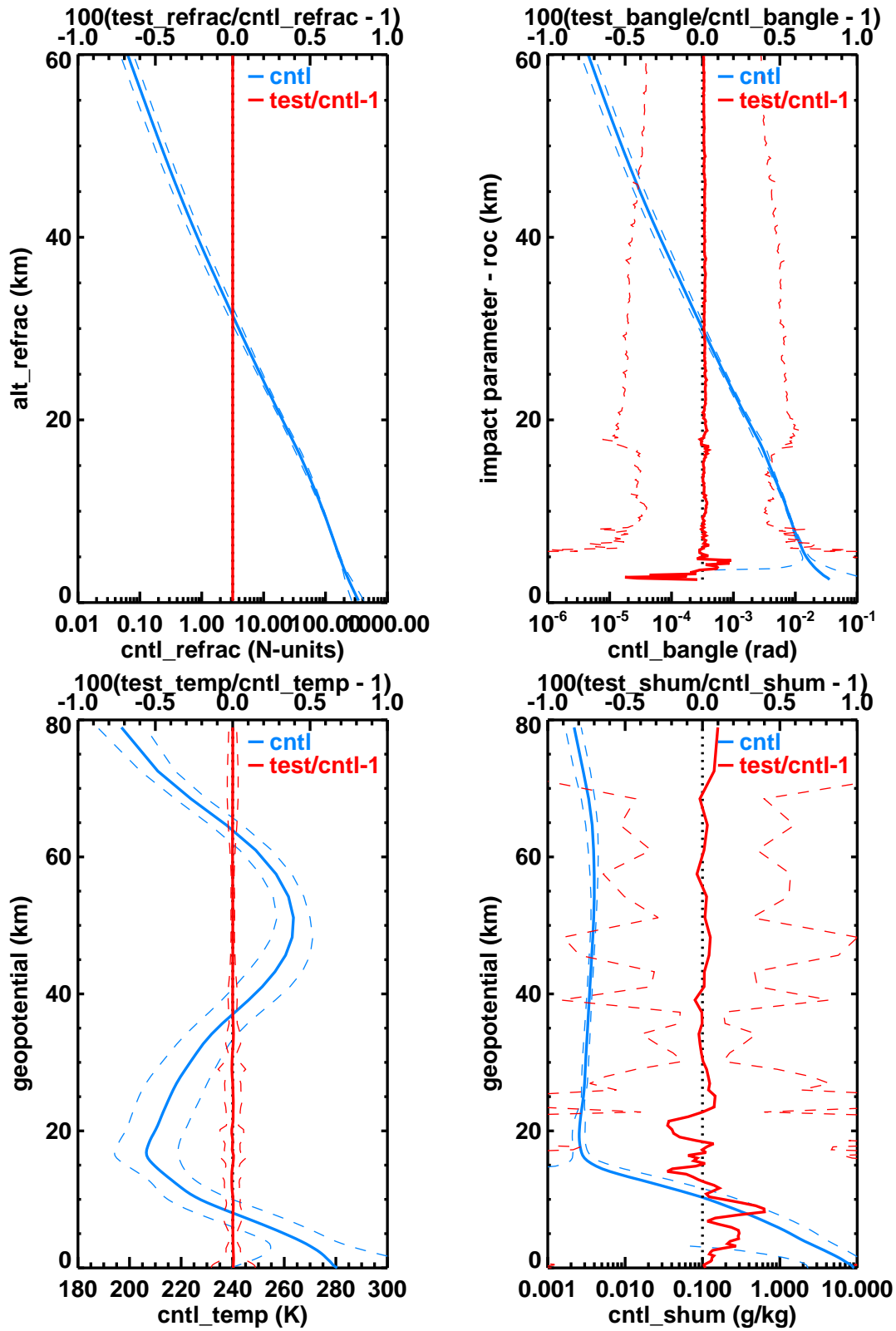


Figure 8.4: Sensitivity of `ropp_fm` and `ropp_ldvar` routines to the undulation. 'cntl' = ROPP expression Eqn (8.7); 'test' = constant value Eqn (8.8). Solid curve = mean, dashed curves = mean \pm one standard deviation.

9 Summary and conclusions

This report has reviewed the geodesy calculations in ROPP as a result of concerns raised by the beta reviewer of ROPP2.0 in 2008. The key findings are as follows.

- The many available expressions for surface gravity differ by no more than 30 parts per million, and often much less;
- Possible values of the (fictitious) effective radius differ by less than 65 parts per million;
- The resulting differences in geopotential heights, or geometric heights, are almost entirely unaffected by differences in the effective radius, and therefore differ by no more than 30 ppm;
- The physical difference between the effective radius R_{eff} and the radius of curvature R_c has been discussed, and the almost constant offset between R_{eff} and $\langle R_c \rangle$ of 21 km has been explained;
- The undulation between the geoid and the ellipsoid, and its spatial variation, have been examined;
- The ROPP-2.0 reviewer's comments have been addressed;
- Studies with ROPP have been undertaken to examine its sensitivity to the quantities discussed in this report.

The overall conclusion is that the geodesy calculations currently available in ROPP (release 6.0) are sufficiently accurate for current purposes.

Acknowledgements

Useful discussions with Huw Lewis, Sean Healy, Christian Marquardt, Chris Burrows, Dave Offiler and John Eyre are gratefully acknowledged. Particular thanks are due to Stig Syndergaard for helping to resolve some of the questions raised in Section 7.

10 Appendix: The geodesy of Rodworld

10.1 Introduction

This Appendix introduces a model which is simple enough to allow analytical studies to be made of the gravitational field around a flattened, rotating body. It is hoped that the results will shed light on some of the more interesting results discussed in the body of the report.

Rodworld consists of a uniform rod of mass M , length $2L$, centred at the origin and lying along the x -axis of a cartesian co-ordinate system. It, and all its observers, rotate at a uniform angular velocity ω about the z -axis.

Rodworld is of course an extreme *prolate* ellipsoid, with major axis in the x -direction, where an extreme *oblate* ellipsoid with minor axis along the z -direction would be more useful. Unfortunately, the latter does not lend itself to easy analytical solutions. Rodworld does at least share with Earth the two key features of flattening and rotation.

The total geopotential, normalised with respect to GM/L , at a point in the plane (x, z) ¹ is derived by integrating point mass sources along the rod, and including the centrifugal potential, and is given by

$$V(x, z) = -1/2 \int_{-L}^L \frac{dx'}{\sqrt{(x-x')^2 + z^2}} - 1/2m'(x/L)^2 \quad (10.1)$$

$$= 1/2 \sinh^{-1}(v_-) - 1/2 \sinh^{-1}(v_+) - 1/2m'(x/L)^2, \quad (10.2)$$

where

$$v_{\pm} = (x \pm L)/z \quad (10.3)$$

and

$$m' = \omega^2 L^3 / GM \quad (10.4)$$

is a normalised rotation rate (squared), whose connection with the rotation parameter m discussed in the body of the report will be discussed in Section 10.3. (Both are proportional to ω^2 .) Note that geopotentials are negative in this sign convention.

The inclusion of the centrifugal potential $-1/2\omega^2 x^2$ in Eqn (10.2) means that the overall gravitational acceleration, normalised with respect to GM/L^2 , is given by the gradient of the total geopotential, thus:

$$\begin{aligned} \mathbf{g}(x, z) = & \left[\frac{(1+v_-^2)^{-1/2} - (1+v_+^2)^{-1/2}}{2z} - m'(x/L) \right] \hat{\mathbf{x}} \\ & + \left[\frac{v_+(1+v_+^2)^{-1/2} - v_-(1+v_-^2)^{-1/2}}{2z} \right] \hat{\mathbf{z}} \end{aligned} \quad (10.5)$$

10.2 Absence of rotation

If $m' = 0$ we can derive some results exactly.

¹We assume $x > 0$ and $z > 0$ to keep things simple, since solutions in other quadrants can always be obtained by symmetry.

10.2.1 Geopotential

By setting $V(x, z) = V_0 = \text{const} < 0$ in Eqn (10.2) it is straightforward if algebraically laborious to establish that the equipotential V_0 occupies the ellipse

$$(x/a_0)^2 + (z/c_0)^2 = 1 \quad (10.6)$$

where

$$a_0 = -L \coth V_0; \quad c_0 = -L \operatorname{csch} V_0 \quad (10.7)$$

which implies

$$a_0^2 = c_0^2 + L^2. \quad (10.8)$$

(Recall that $V_0 < 0$.) Thus, for example, the geopotential $V = V_0 = \sinh^{-1}(-1) = -\log(1 + \sqrt{2}) \approx -0.88$ passes through $(\sqrt{2}L, 0)$ and $(0, L)$. It, and two of its neighbouring geopotentials, is shown in the top panel of Fig 10.1. It is immediately clear that the local gravity, which is inversely proportional to the spacing between the geopotentials, is *weaker* at the pole than at the equator — despite the pole being nearer Rodworld's centre of mass. This possibly surprising result, stressed in a contrary context² by White et al ([16]), is clearly a subtle consequence of the *distribution* of the mass that generates the geopotentials.

10.2.2 Surface gravity

The orthogonality of the geopotential V and reduced (or parametric) latitude β , defined by

$$x = a \cos \beta; \quad z = c \sin \beta, \quad (10.9)$$

makes it convenient to express the magnitude of the gravity, normalised with respect to GM/L^2 , as a function of latitude β and geopotential V , as follows:

$$g(V, \beta) = \frac{\sinh^2 V}{\sqrt{1 + \sin^2 \beta \sinh^2 V}}. \quad (10.10)$$

(The reduced latitude β is related to the geodetic latitude ϕ by $\tan \beta = (c/a) \tan \phi$. On Earth, the maximum difference between the two latitudes is about 0.1° at $\phi \approx \pm 45^\circ$. They agree at the pole and the equator, of course.)

$g(V, \beta)$ is clearly a decreasing function of latitude and altitude (because the $|V|$ gets smaller as distance from the origin increases). Along a general latitude line it does not follow the strict inverse square law of Eqn (3.1). In particular,

$$g_{\text{eq}} = g(V, 0) = \sinh^2 V = (1 - f)^{-2} - 1 \quad (10.11)$$

$$\approx 2f(1 + 3f/2) \quad \text{for } f \ll 1, \quad (10.12)$$

$$g_{\text{po}} = g(V, \pi/2) = \sinh^2 V / \cosh V = (1 - f)^{-1} - (1 - f) \quad (10.13)$$

$$\approx 2f(1 + f/2) \quad \text{for } f \ll 1, \quad (10.14)$$

where the flattening f is defined as

$$f = (a - c)/a. \quad (10.15)$$

²i.e. that confocal oblate ellipsoids could *not* represent equipotentials on the rotating earth, where $g_{\text{po}} > g_{\text{eq}}$, for this reason.

It immediately follows that the ratio of the polar to equatorial gravity is

$$g_{po}/g_{eq} = \operatorname{sech} V = c/a = 1 - f, \quad (10.16)$$

by extension of Eqn (10.7) to a general geopotential V . Eqn (10.16), which is *exact*, matches Clairaut's first order result, Eqn (2.19), in the absence of rotation.

Thus, for example, the magnitude of polar gravity on the equipotential surface $V = V_0 = -\log(1 + \sqrt{2}) \approx -0.88$ (which cuts the z -axis at L) is $1/\sqrt{2}$, while the equatorial gravity on the same geopotential (which cuts the x -axis at $\sqrt{2}L$) is 1. Equatorial gravity only falls to $1/\sqrt{2}$ at $x = \sqrt{1 + \sqrt{2}}L$.

The 'isograv' $g(x, z) = g_0 = 1/\sqrt{2}$, and two of its neighbours, is shown on the bottom panel of Fig 10.1. That the isogravs are flatter than the equipotentials is clear. This leads to the reduction in gravity towards the pole, as expressed by Eqn (10.10).

Fig 10.1 depicts the situation when $f \sim 1$. On Earth, however, we know that $f \approx 1/300$. This implies, from Eqn (10.7), that the equivalent normalised geopotential in Rodworld is $V = -\tanh^{-1}(\sqrt{f(2-f)}) \approx -\sqrt{2f} \approx -8.2 \times 10^{-2}$ — which is coincidentally the eccentricity of the ellipse. Thus, if we wish to use Rodworld to model the Earth, then the appropriate dimensionless geopotentials are numerically very small. In this case we would also have (from Eqn (10.7)) $a/L \approx c/L \approx -1/V \approx 12$. Hence a 1000 km long rod, with the same mass as the Earth, would have the same gravitational effect as the Earth at its surface ($r \sim 6400$ km). The highly flattened geopotentials sketched in Fig 10.1, where $|V| \sim 1$, would therefore represent the situation far beneath the surface of this 'rod and shell' model of the Earth.

In terms of f , Eqn (10.10) says

$$g(V, \beta) = \frac{f(2-f)}{(1-f)\sqrt{(1-f)^2 + f(2-f)\sin^2\beta}} \quad (10.17)$$

$$\approx 2f(1 + (3/2 - \sin^2\beta)f) \quad \text{for } f \ll 1. \quad (10.18)$$

Given that this g is normalised with respect to GM/L^2 , we find that, in the small V (and therefore f) limit, the unnormalised gravity, \tilde{g} , is given by

$$\tilde{g}(V, \beta) \approx (GM/c^2)(1 - f\sin^2\beta) \quad \text{for } f \ll 1, \quad (10.19)$$

which is the same limiting form (in the absence of rotation) as the equations in Section 2, such as Lambert's equation (2.1) or Somigliana's equation (2.5), as used in ROPP. Note the vaguely interesting implications that $\tilde{g}_{eq} = (GM/c^2)$, not (GM/a^2) , and that $\tilde{g}_{po} = (GM/ac)$, not (GM/c^2) . These again are a consequence of the *distribution* of mass along the rod.

10.2.3 Effective radius

As discussed in Section 3, the effective radius encodes the rate of change of gravity with height, g_h , in order that the variation of gravity with latitude and altitude can be expressed by means of Eqn (3.1). g_h is calculated thus:

$$g_h = \partial g / \partial h = (\partial g / \partial V)(\partial V / \partial h) = g \partial g / \partial V = 1/2 \partial g^2 / \partial V \quad (10.20)$$

since $g = \partial V / \partial h$. We therefore obtain

$$g_h(V, \beta) = \frac{2 \sinh^3 V \cosh V (1 + 1/2 \sin^2 \beta \sinh^2 V)}{L(1 + \sin^2 \beta \sinh^2 V)^2}. \quad (10.21)$$

Eqns (10.10) and (10.21) imply in particular that

$$ag_h(V, 0)/g_{\text{eq}} = -2(1-f)^{-2} \quad (10.22)$$

$$\approx -2(1+2f) \quad \text{for } f \ll 1, \quad (10.23)$$

$$ag_h(V, \pi/2)/g_{\text{eq}} = -(1+(1-f)^2) \quad (10.24)$$

$$\approx -2(1-f) \quad \text{for } f \ll 1 \quad (10.25)$$

and in general that

$$ag_h(V, \beta)/g_{\text{eq}} \approx -2(1+2f-3f\sin^2\beta) \quad \text{for } f \ll 1. \quad (10.26)$$

This is not quite in agreement with the International Gravity Formula (IGF, Eqn (2.20)), which says, in this limit,

$$ag_h(V, \beta)/g_{\text{eq}} \approx -2(1+f-3f\sin^2\beta) \quad \text{for } f \ll 1. \quad (10.27)$$

We can go further and calculate the second derivative of g on Rodworld with respect to h . The full expression is too messy to reproduce, but the limit as $V, f \rightarrow 0$ is worth recording:

$$a^2g_{hh}(V, \beta)/g_{\text{eq}} \approx 6(1+14/3f-6f\sin^2\beta) \quad \text{for } f \ll 1. \quad (10.28)$$

Again, this is not quite in agreement with the International Gravity Formula, which says, in this limit,

$$a^2g_{hh}(V, \beta)/g_{\text{eq}} \approx 6(1+7/3f-6f\sin^2\beta) \quad \text{for } f \ll 1. \quad (10.29)$$

It remains to be seen whether these differences from the International Gravity Formula can be — or need to be — reconciled. After all, Rodworld and Earth even have different dimensions. Note, however, that the IGF gives the ‘correct’ expression for the effective radius in the low f limit. For, as in Section 3, the above expressions for g and g_h can be combined to give the effective radius

$$R_{\text{eff}}(V, \beta) = -2g(V, \beta)/g_h(V, \beta) \quad (10.30)$$

$$= -L \frac{(1 + \sin^2\beta \sinh^2 V)^{3/2}}{\sinh V \cosh V (1 + 1/2 \sin^2\beta \sinh^2 V)}. \quad (10.31)$$

This implies in particular that

$$R_{\text{eff}}(V, 0)/a = (1-f)^2 \quad (10.32)$$

$$\approx (1-2f) \quad \text{for } f \ll 1, \quad (10.33)$$

$$R_{\text{eff}}(V, \pi/2)/a = 2/((1-f) + (1-f)^{-1}) \quad (10.34)$$

$$\approx 1 \quad \text{for } f \ll 1 \quad (10.35)$$

and in general that

$$R_{\text{eff}}(V, \beta)/a \approx (1-2f\cos^2\beta) \quad \text{for } f \ll 1. \quad (10.36)$$

In contrast, the IGF (Eqn (2.20)) implies

$$R_{\text{eff}}(V, \beta)/a \approx (1+f-2f\cos^2\beta) \quad \text{for } f \ll 1, \quad (10.37)$$

which is the same (in the absence of rotation) as Eqn (3.7), the first order expansion of the expression Eqn (3.4), which is used in ROPP.

In either case, the key finding that R_{eff} *increases* with latitude should be noted.

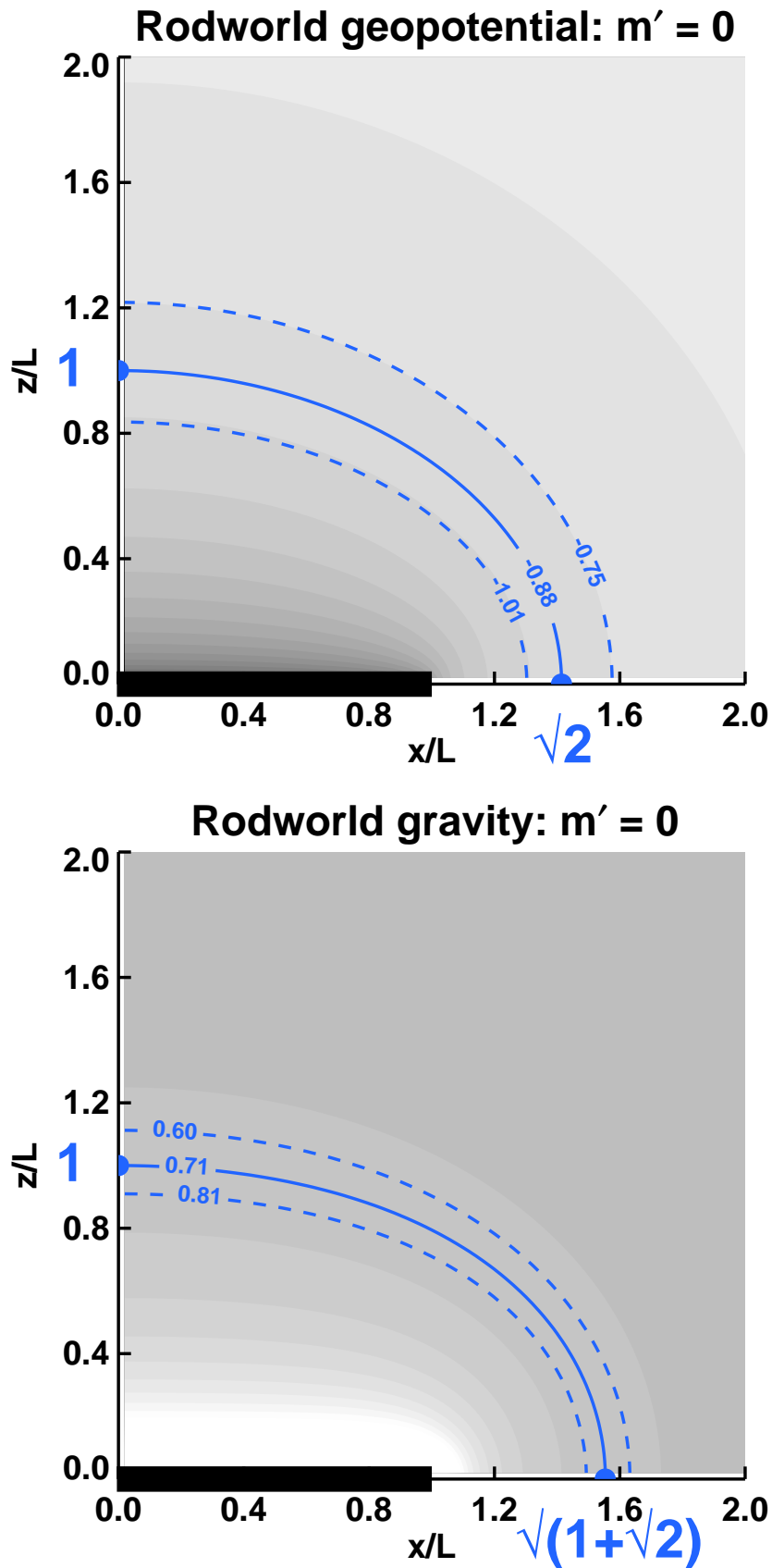


Figure 10.1: Geopotentials (top) and constant gravity contours (bottom) in a non-rotating Rodworld. Solid lines show position of equipotential $V = V_0 = -\log(1 + \sqrt{2})$ and isograv $g = g_0 = 1/\sqrt{2}$. Dashed lines indicate neighbouring geopotentials and isogravs.

10.3 Presence of rotation

On Earth we know that $m = \omega^2 a / g_{\text{eq}} \approx 1/300 \ll 1$. Since $m' = \omega^2 L^3 / GM \sim (L/a)^3 m$ and $L/a \sim 1/12$ when we use Rodworld to simulate the Earth's gravitational field (see Section 10.2.2), it follows that $m' \ll 1$. We should therefore be able to treat m' perturbatively.

This long and involved calculation would fill an Appendix to this Appendix, which is probably taking things too far, particularly when we can evaluate the general expressions (10.2) and (10.5) numerically, and key expressions can be evaluated at the equator and the pole analytically.

10.3.1 Geopotential

The equipotential $V(x, z) = V_0$ which, in the absence of rotation, cut the z -axis at $c_0 = -L \operatorname{csch} V_0$ and the x -axis at $a_0 = -L \operatorname{coth} V_0$, now crosses the x -axis at

$$a'_0 = a_0 [1 + (m'/2) \operatorname{csch}^2 V_0] \quad \text{to first order in } m' \quad (10.38)$$

$$= a_0 [1 + (m/2)(1-f)^2 \sqrt{f(2-f)}] \quad \text{to first order in } m, \quad (10.39)$$

which implies that the revised flattening $f' = (a'_0 - c_0)/a'_0$ is given by

$$f' = f + (m'/2) \operatorname{sech} V_0 \operatorname{csch}^2 V_0 \quad \text{to first order in } m \quad (10.40)$$

$$= f + (m/2)(1-f)^3 \sqrt{f(2-f)} \quad \text{to first order in } m \quad (10.41)$$

$$= f \quad \text{to first order in } f \text{ and } m \quad (10.42)$$

The equipotentials are therefore flattened a little by rotation.

The geopotentials for $m' = 0.1$ are sketched in the top panel of Fig 10.2. Comparison with Fig 10.1 shows the degree to which rotation has flattened the equipotentials. It is also clear that gravity, inversely proportional to the geopotential spacing, is now *smaller* at the equator than at the pole. This is what Clairaut's equation, Eqn (2.19), would suggest for sufficiently large m .

10.3.2 Surface gravity

The constant gravity contours for $m' = 0.1$ are sketched in the bottom panel of Fig 10.2. Comparison with Fig 10.1 shows that the centrifugal acceleration caused by rotation has, of course, weakened gravity at the equator. We can show that, to first order in m throughout,

$$g(V, 0) = ((1-f)^{-2} - 1) \{1 - m[(1-f)^2 + \sqrt{f(2-f)}]\} \quad (10.43)$$

$$\approx 2f(1 + 3f/2 - m) \quad \text{for } f, m \ll 1, \quad (10.44)$$

$$g(V, \pi/2) = (1-f)^{-1} - (1-f) \quad (10.45)$$

$$\approx 2f(1 + f/2) \quad \text{for } f \ll 1, \quad (10.46)$$

which together imply

$$g_{\text{po}}/g_{\text{eq}} \approx 1 + m - f \quad \text{for } f, m \ll 1, \quad (10.47)$$

which is the Rodworld analogue of Clairaut's equation (which is reproduced by the IGF). On Earth, as it is in Rodworld, m and f have opposing tendencies in this expression.

In Fig 10.2, $m' = 0.1$ and $f \approx 1 - 1/\sqrt{2} \sim 0.3$, which means that $m = m'(f(2-f))^{-3/2} \sim 0.3$, so that we might expect polar and equatorial gravities to be about the same. In fact, because we cannot really neglect terms of second order in f here, gravity is actually slightly larger at the pole than at the equator. As on Earth, the rotation effect dominates the flattening effect here.

10.3.3 Effective radius

We find on Rodworld that

$$\begin{aligned} ag_h(V, 0) &= -2(1-f)^{-2}((1-f)^{-2} - 1)\{1 - (m/2)[(4 - (1-f)^2)\sqrt{f(2-f)} - (1-f)^4]\} \quad (10.48) \\ &\approx -4f(1+7f/2)(1 - (m/2)(3\sqrt{2f} - 1)) \quad \text{for } f \ll 1 \quad (10.49) \end{aligned}$$

$$ag_h(V, \pi/2) = -((1-f)^{-2} + (1-f)^2) \quad (10.50)$$

$$\approx -4f(1+f/2) \quad \text{for } f \ll 1. \quad (10.51)$$

Eqns (3.2), (10.43), (10.45), (10.48) and (10.50) imply that

$$\begin{aligned} R_{\text{eff}}(V, 0)/a &= (1-f)^{-2}\{1 - (m/2)[((1-f)^2 - 2)\sqrt{1 - (1-f)^2} + 2(1-f)^2 + (1-f)^4]\} \quad (10.52) \\ &\approx 1 - 2f - 3m/2 \quad \text{for } f \ll 1 \quad (10.53) \end{aligned}$$

$$R_{\text{eff}}(V, \pi/2)/a = 2/((1-f) + (1-f)^{-1}) \quad (10.54)$$

$$\approx 1 \quad \text{for } f \ll 1. \quad (10.55)$$

In contrast, the IGF (Eqn (2.20)) implies

$$R_{\text{eff}}(V, \beta)/a \approx (1 + f - m - 2f \cos^2 \beta) \quad \text{for } f \ll 1, \quad (10.56)$$

which further implies

$$R_{\text{eff}}(V, 0)/a \approx (1 - f - m) \quad \text{for } f \ll 1 \quad (10.57)$$

$$R_{\text{eff}}(V, \pi/2)/a \approx (1 + f - m) \quad \text{for } f \ll 1. \quad (10.58)$$

Close agreement was always unlikely, but at least the signs of the terms in f and m tally. And since $f \approx m$ for the Earth, the effective radius at the pole also approximately equals that of Rodworld (namely, a), and this suggests how to partially reconcile the expressions. The semi-major axis a in Eqns (10.55) is the *unperturbed* value. As discussed in Section 10.3.1, rotation increases this a little, so that the real semi-major axis a' is given by Eqn (10.39). Hence, the effective radius at the pole is *less* than a' by a term proportional to m — just as the IGF would say. (Unlike the terrestrial situation, however, for Rodworld the coefficient of m is multiplied by \sqrt{f} , so the rationalisation is only qualitative.)

Once again, the key result is that, on Rodworld and on Earth, the effective radius is *greater* at the pole than at the equator.

10.4 Summary

Rodworld is a simple model of a rotating, non-spherically symmetric system with flattened geopotentials. Its simplicity allows analytical progress to be made in the study of some of the more interesting aspects of the geodesy of the Earth, such as the *reduction* in gravity with latitude in the absence of rotation. Some aspects are even in quantitative agreement with their terrestrial counterparts.

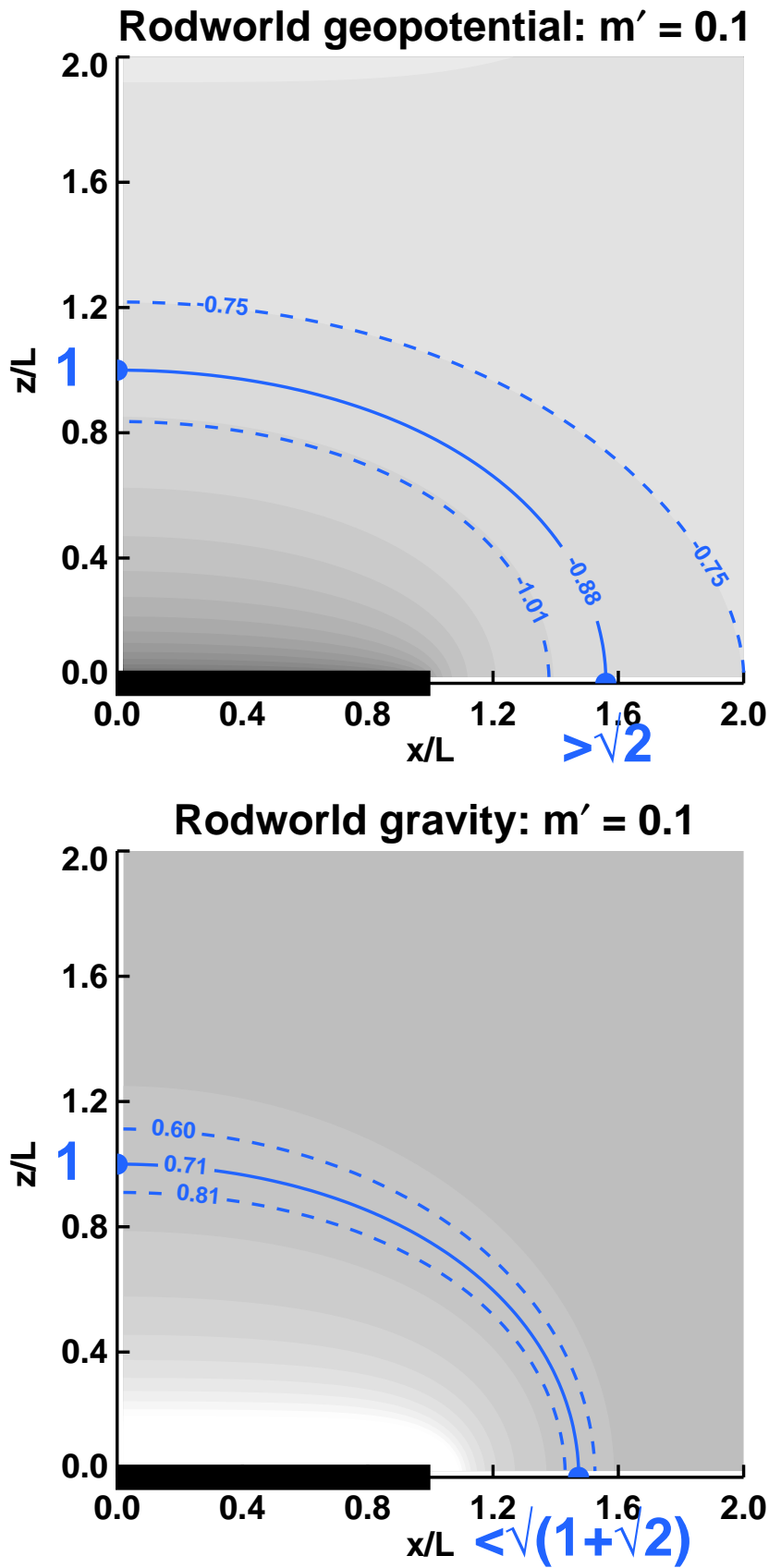


Figure 10.2: Geopotentials (top) and constant gravity contours (bottom) in a rotating Rodworld. Solid lines show position of equipotential $V = V_0 = -\log(1 + \sqrt{2})$ and isograv $g = g_0 = 1/\sqrt{2}$. Dashed lines indicate neighbouring geopotentials and isogravs.

Bibliography

- [1] GRAS SAF, ROPP-2 Beta Test Report, SAF/GRAS/METO/TR/ROPP/002, 2008.
- [2] Heiskanen and Moritz, Physical Geodesy, W H Freeman and Co., 1967.
- [3] Kursinski E R, Hajj G A, Leroy S S and Herman B, The GPS Radio Occultation Technique, Terrestrial, Atmospheric and Oceanic Sciences, **11**, 1, pp53-114, 2000.
- [4] Lambert, The International Gravity Formula,
<http://earth.geology.yale.edu/ajs/1945A/360.pdf>, 1945.
- [5] Lambert, Gravity formulas for meteorological purposes. A discussion prepared in response to a request of the International Meteorological Organisation, pamphlet available from National Meteorological Library, Exeter, UK, 1948.
- [6] Lewis, Geodesy calculations in ROPP, GRAS SAF Report 02, SAF/GRAS/METO/REP/GSR/002, 2007.
- [7] Li and Götze, Tutorial: Ellipsoid, geoid, gravity, geodesy and geophysics,
http://www.fugro-gravmag.com/resources/Technical_Papers/Li_Goetze_Geophysics_2001.pdf, 2001.
- [8] Mahoney, A Discussion of Various Measures of Altitude,
<http://mtp.jpl.nasa.gov/notes/altitude/altitude.html>, 2008.
- [9] Mahoney, An Exact Expression for Normal Gravity,
<http://mtp.jpl.nasa.gov/notes/altitude/Gnormal.html>, 2008.
- [10] NASA, <http://cddis.nasa.gov/926/egm96/egm96.html>, 2004.
- [11] National Geospatial-Intelligence Agency,
<http://earth-info.nga.mil/GandG/wgs84/index.html>, 2010.
- [12] Offiler, Calculation of the undulation in ROPP, ROM SAF Report 15, SAF/ROM/METO/REP/RSR/015, 2013.
- [13] Rodgers, Inverse Methods for Atmospheric Sounding - Theory and Practice, World Scientific., 2000.
- [14] Smithsonian meteorological tables,
http://openlibrary.org/books/OL7107344M/Smithsonian_meteorological_tables, 1896.
- [15] Syndergaard, Modeling the impact of the Earth's oblateness on the retrieval of temperature and pressure profiles from limb sounding, Journal of Atmospheric and Solar-Terrestrial Physics, **60**, pp171-180, 1998.
- [16] White A A, Staniforth A and Wood N, Spheroidal coordinate systems for modelling global atmospheres, Quart. Jour. Royal Met. Soc., **134**, 261-270, 2008.

ROM SAF (and GRAS SAF) Reports

SAF/GRAS/METO/REP/GSR/001	Mono-dimensional thinning for GPS Radio Occultation
SAF/GRAS/METO/REP/GSR/002	Geodesy calculations in ROPP
SAF/GRAS/METO/REP/GSR/003	ROPP minimiser - minROPP
SAF/GRAS/METO/REP/GSR/004	Error function calculation in ROPP
SAF/GRAS/METO/REP/GSR/005	Refractivity calculations in ROPP
SAF/GRAS/METO/REP/GSR/006	Levenberg-Marquardt minimisation in ROPP
SAF/GRAS/METO/REP/GSR/007	Abel integral calculations in ROPP
SAF/GRAS/METO/REP/GSR/008	ROPP thinner algorithm
SAF/GRAS/METO/REP/GSR/009	Refractivity coefficients used in the assimilation of GPS radio occultation measurements
SAF/GRAS/METO/REP/GSR/010	Latitudinal Binning and Area-Weighted Averaging of Irregularly Distributed Radio Occultation Data
SAF/GRAS/METO/REP/GSR/011	ROPP 1dVar validation
SAF/GRAS/METO/REP/GSR/012	Assimilation of Global Positioning System Radio Occultation Data in the ECMWF ERA-Interim Re-analysis
SAF/GRAS/METO/REP/GSR/013	ROPP PP validation
SAF/ROM/METO/REP/RSR/014	A review of the geodesy calculations in ROPP
SAF/ROM/METO/REP/RSR/015	Improvements to the ROPP refractivity and bending angle operators

ROM SAF Reports are accessible via the ROM SAF website: <http://www.romsaf.org>